# EXPLORING THE RELATIONSHIP BETWEEN N-ACETYLASPARTATE AND WHITE MATTER INTEGRITY IN SCHIZOPHRENIA: A 7T ($^{1}$H) MRS-DTI APPROACH

By

Dominic Trevor Roberts

A THESIS

Submitted to
Michigan State University
in partial fulfillment of the requirements
for the degree of

Psychology --- Master of Arts

2021

## ABSTRACT

EXPLORING THE RELATIONSHIP BETWEEN N-ACETYLASPARTATE AND WHITE MATTER INTEGRITY IN SCHIZOPHRENIA: A 7T ($^1$H) MRS-DTI APPROACH

By

Dominic Trevor Roberts

Altered brain connectivity is a potential physiological mechanism of schizophrenia. Compromised white matter has been reported in schizophrenia; however, few studies have investigated the neurochemical abnormalities underlying these microstructural differences. N-acetylaspartate is often reduced in persons with schizophrenia (SZ) and their unaffected first-degree relatives (REL) and is a potential mechanism underlying these white matter abnormalities. We used a combined MRS-DTI approach to investigate the relationship between NAA and white matter integrity in SZ, REL, and healthy controls (HC).

49 HC, 23 REL and 23 SZ underwent 7T proton magnetic resonance spectroscopy and 3T diffusion tensor imaging. NAA concentrations in the visual cortex and basal ganglia were measured and compared across groups. Tract-based spatial statistics were used to derive and compare fractional anisotropy (FA), axial diffusivity (AD), mean diffusivity (MD) and radial diffusivity (RD) across groups. NAA concentrations were then correlated to these measures.

Visual cortex NAA was significantly reduced in SZ compared to HC but not REL. No group differences were observed in any measure of white matter integrity. Reduced NAA concentrations in the visual cortex and basal ganglia correlated with diffusivity measures that were generally consistent with poor white matter microstructure. These data suggest that NAA concentrations may be related to white matter integrity.

## ACKNOWLEDGEMENTS

I would like to thank my mentor, Dr. Katharine Thakkar, and my Masters committee members, Dr. Alex Johnson and Dr Jason Moser, for their support and feedback on this project.

## TABLE OF CONTENTS

## LIST OF TABLES

## LIST OF FIGURES

# INTRODUCTION

Schizophrenia is a severe, chronic psychological disorder characterized by the experience of hallucinations, delusions, disorganized thinking and negative symptoms (e.g. blunted affect and low motivation). Affecting over 20 million people worldwide (WHO, 2019), schizophrenia carries significant psychological and physical health burden, reducing the life expectancy of those it affects by 15 years (Hjorthøj et al., 2017). Whilst pharmacological agents are available to treat schizophrenia and are effective in stabilizing symptoms for some patients (Patel et al., 2014), risk of relapse is high with less than 15% of patients achieving a sustained reduction in symptoms (Jääskeläinen et al., 2013).

Despite obvious limited efficacy, the development of new medications for schizophrenia is slow and hampered by the lack of theoretical frameworks that recognize the extreme heterogeneity in symptom presentation and disease progression in persons with schizophrenia (Habtewold et al., 2020). Indeed, even at the neural level, observable structural and volumetric gray matter differences of specific brain regions overlap in just 2% of patients (Wolfers et al., 2018) suggesting that theories which focus on explaining schizophrenia in terms of disruptions to global brain processes may better capture the symptomatology of schizophrenia. One such theory, the dysconnection hypothesis, posits that schizophrenia is a disorder of brain connectivity (Friston et al., 1998) whereby the symptoms of psychosis are the result of inefficient, or aberrant, functional integration across brain regions (Stephan et al., 2009).

Although the causes of this abnormal functional integration remain unknown, impairments in myelin sheathing are a likely candidate. A product of oligodendrocytes, myelin is a fatty substance which forms white matter and insulates axons to enable rapid, synchronized communication in the brain (Nickel & Gu, 2018). Evidence of myelin dysfunction in

schizophrenia is supported by post-mortem studies of persons with schizophrenia which have found reduced numbers of oligodendrocytes (Uranova et al., 2004, 2007), reduced expression of myelin-related proteins (Matthews et al., 2012) and increased incidence of myelin abnormalities (Flynn et al., 2003; Walker et al., 2018). Furthermore, diffusion tensor imaging (DTI) studies have reported in vivo evidence of reduced white matter integrity and volume in persons with schizophrenia (Haijma et al., 2013; Kelly et al., 2018; Vitolo et al., 2017; Yao et al., 2013) and their unaffected first-degree relatives (Boos et al., 2007; Camchong et al., 2009; de Zwarte et al., 2019; Prasad et al., 2015). Thus, evidence of white matter abnormalities in persons with schizophrenia appears to be robust and consistent. That these abnormalities exist in first-degree relatives also suggests that these alterations reflect a vulnerability to schizophrenia rather than a consequence of the illness.

Whilst DTI measures can only detect a specific white matter abnormalities in schizophrenia, research using other neuroimaging techniques suggest that compromised myelin may be driving these findings. Indeed, studies using T2 relaxation imaging have reported evidence of reduced, or abnormal, myelination in persons with schizophrenia (Du et al., 2013; Flynn et al., 2003; Lang et al., 2014; Vanes et al., 2018, 2019). Therefore, it seems likely that the white matter abnormalities observed in persons with schizophrenia are related to compromised myelination.

But what is the mechanism that contributes to these putative myelination abnormalities? The synthesis and repair of myelin by oligodendrocytes require acetate which is primarily derived from a neurometabolite known as n-acetylaspartate (NAA). NAA's role in myelin synthesis is well-documented and NAA has been implicated in several white matter disorders (see Moffett et al., 2007 for review), suggesting that NAA could be a promising candidate for

understanding the white matter abnormalities in schizophrenia. Concentrations of NAA can be measured in-vivo using magnetic resonance spectroscopy (MRS). Studies using MRS have observed reduced concentrations of neural NAA in persons with schizophrenia (Brugger et al., 2011; Iwata et al., 2018; Marsman et al., 2013; Reid et al., 2013; Steen et al., 2005) and their unaffected first-degree relatives (Fuente-Sandoval et al., 2011; Keshavan et al., 2009; Tandon et al., 2013). Thus, reductions in neural NAA may underly the dysconnectivity associated with schizophrenia, via its effects on myelin production and repair.

Despite robust evidence supporting white matter abnormalities and reduced NAA concentrations in persons with schizophrenia, few studies have examined the relationship between concentrations of NAA and white matter integrity in schizophrenia. In those that have, lower NAA concentrations have predicted greater reductions in white matter integrity (Reid et al., 2016; Steel et al., 2001; Tang et al., 2007). However, methodological concerns limit the interpretability of these studies. For example, existing studies calculated concentrations of NAA as a ratio of a comparison metabolite (e.g. NAA may be quantified as a ratio of NAA to creatine, NAA/CR). This is troublesome because a reduction in NAA quantified in this manner could be driven by a reduction in NAA, an increase in the denominator metabolite (creatine, in this example), or a combination of both. Furthermore, previous studies examining NAA-white matter relationships have depended on recruitment of medicated patient samples, which calls into question whether observed changes in white matter or NAA, are due to medication, are a mechanism of the illness, or whether they reflect a general vulnerability to schizophrenia.

We aimed to address these limitations by examining the relationship between concentrations of NAA and white matter integrity in persons with schizophrenia and their first-degree relatives. In order to circumvent confounds related to NAA quantification, we referenced

NAA concentrations with respect to water, thereby avoiding the need for comparison metabolites. NAA concentrations were correlated to measures of white matter integrity derived from DTI. Additionally, we examined the relationship between NAA and white matter integrity in the unaffected siblings of persons with schizophrenia. To our knowledge, no other combined DTI-MRS study has examined the relationship between NAA and white matter integrity in first degree relatives of schizophrenia, thus allowing us to make inferences into whether putative NAA-white matter relationships represent a general vulnerability towards schizophrenia or are related to mechanisms related to the disease itself (e.g., a proximal illness mechanism), or are side-effects of medication use.

We hypothesized that reduced concentrations of NAA would predict the reductions in white matter integrity typically observed in persons with schizophrenia. As such, we predicted that individuals with schizophrenia, and their first-degree relatives, would show reduced white matter integrity relative to healthy controls. Furthermore, we predicted that individuals with schizophrenia, and their first-degree relatives, would show reduced concentrations of NAA compared to healthy controls. Finally, we predicted that NAA concentrations would correlate with measures of white matter integrity, such that lower NAA concentrations would predict reduced white matter integrity.

## METHOD

### Participants

All subjects were recruited as part of a larger study where participants were invited to participate in two scan sessions (one in which DTI scans were acquired and one in which MRS scans were acquired). The total sample comprised 95 individuals. Participants were included in this study if they had useable MRS data, useable DTI data or both.

The MRS portion of the study was completed by 68 participants, 21 of whom were persons with schizophrenia or schizoaffective disorder (SZ), 23 were unaffected healthy siblings of persons with schizophrenia (REL) who had no personal history of DSM-IV Axis 1 disorders and 24 were unrelated healthy controls (HC) of either sex who reported no personal history of DSM-IV Axis 1 disorders or familial history of schizophrenia spectrum disorders. Furthermore, 86 participants underwent 3T DTI. Of these, there were 22 SZ, 20 REL and 44 HC. Participants in all groups were aged between 18-55 and were excluded from participation if they had a history of significant head trauma or neurologic illness and substance dependence or abuse within 6 months of the study. Demographic data for the MRS and DTI samples are shown in table 1 and table 2, respectively.

Diagnoses for the SZ and REL groups were based upon clinician interviews using the Comprehensive Assessment of Symptoms and History interview (CASH; Andreasen, Flaum & Arndt(1992)) or Schedules for Clinical Assessment for Neuropsychiatry (SCAN; Wing et al., 1990). All patients were taking antipsychotic medication at the time of participation. Chlorpromazine equivalent antipsychotic doses were calculated for every patient. Clinical symptoms of patients were measured using the Positive and Negative Syndrome Scale (PANSS; Kay, Fiszbein & Opler (1987)).

Each participant's IQ was measured using the Dutch equivalent of the National Adult Reading Test (NVIQ; Schmand, Bakker, Saan & Louman, 1991) and handedness was measured with the Edinburgh Handedness Inventory (Oldfield, 1971). Groups were matched on gender, handedness, and IQ for both the MRS and DTI samples. HC and REL had more years of education compared to SZ in both the MRS and DTI samples**.** REL were significantly younger than SZ for MRS data, and both REL and HC were significantly younger than SZ in our DTI sample.

Study procedures were approved by the Human Ethics Committee of the University Medical Center, Utrecht, The Netherlands. All participants provided written informed consent and received compensation for their participation.

**Magnetic Resonance Spectroscopy**

A 7T whole-body MR scanner (Philips Medical Systems, Cleveland, OH) was used to acquire $^{1}$H-MRS and anatomic images in a single scan session for each participant as described previously (Thakkar et al., 2017). Furthermore, given the ability for superior tissue classification, a 3T scanner was used to acquire high-resolution T1-weighted anatomic images in a second session, which were subsequently used for segmenting the 1H-MRS voxel into different tissue types.

***Acquisition***

A dual-transmit birdcage head coil (Nova Medical, Inc., Wilmington, MA) was used in combination with a 32-channel receive coil (Nova Medical, Inc.) in the 7T MR scanner. A T1-weighted magnetization prepared rapid acquisition gradient-echo sequence was acquired for voxel placement (174 slices, echo time [TE] = 1.8 ms, repetition time [TR] = 4 ms, flip angle = 71, field of view = 246 x 246 x 174 mm). A semilocalized by adiabatic selective refocusing

sequence (TE = 36 ms, TR = 5000 ms, 32 averages, maximum B1 = 17 mT) was used to measure NAA. To optimize phase settings of the individual transmit channels we used radiofrequency shimming on the region of interest before MRS acquisition. This allowed a B1 of 17mT to be reached, thus minimizing the chemical shift displacement artifacts in the voxel of measurement. Before MRS acquisition, second order B0 shimming was automatically applied.

We obtained conventional spectra from three voxels (40 x 24 x 25 mm) which were placed in the left and right basal ganglia, including as much striatum as possible but avoiding lateral ventricles, and the bilateral visual cortex, centered on the calcarine sulcus (Figure 1). In the 3T Philips Achieva MR scanner (Philips Medical Systems, Best, The Netherlands), a whole-brain three-dimensional fast field echo T1-weighted scan (200 slices, TR = 10 ms, TE = 4.6 ms, flip angle = 81, field of view = 240 x 240 x 160 mm, voxel size = 0.75 x 0.8 x 0.75 mm) was acquired using an eight-channel head coil.

Although data were acquired in the bilateral basal ganglia, the signal in the left basal ganglia was particularly poor for many participants. Given there were no hypotheses regarding laterality differences in basal ganglia NAA, only data from the right basal ganglia and visual cortex are reported in this paper (see Thakkar et al. (2017) for a discussion of the poor left basal ganglia signal quality observed in this sample).

***Processing***

For data in each measurement voxel, the 32 receiver coils were combined after amplitude weighting and phasing based on the water reference signal and noise decorrelation based on a noise scan. The water reference was also used for eddy current correction and as an internal standard for quantification. Conventional MR spectra were quantified using an LCModel based software implemented in MATLAB NMR Wizard (MATLAB; The MathWorks, Inc., Natick,

MA; de Graaf RA (1998)), which relies on a priori knowledge of the spectral components of metabolites to fit metabolite profiles. A measured macromolecular profile and the following simulated metabolite profiles were fitted to each spectrum: taurine, myo-inositol, glutathione, Gln, Glu, GABA, N-acetylaspartylglutamate, N-acetylaspartate, phosphocreatine, creatine, phosphoethanolamine, glycerophosphocholine, phosphocholine, choline, aspartate, and acetate (figure 2). The macromolecular baseline was acquired in the prefrontal cortex and averaged across four healthy individuals who did not participate in the present study, using the same semi localized by adiabatic selective refocusing sequence with inversion recovery (Pfeuffer, Tkák, Provencher & Gruetter (1999)). The baseline of the fit was adjusted to incorporate possible lipid and water artifacts.

***Exclusion Criteria***

Individual metabolite concentrations were excluded based on the following spectral quality criteria: 1) Mean-scaled Cramer-Rao lower bound (CRLB) values ≥ 20 (Near, 2013) and 2) linewidth >26 hz. Mean-scaled CRLB values are reported in line with the recommendations of (Kreis, 2016) who suggests that thresholding based on absolute CRLB values can inappropriately distort data. These values were calculated by dividing a participant's absolute CRLB value for NAA by the mean NAA concentration of healthy controls.

Due to a bug in data acquisition code, the measurement voxel for the visual cortex was erroneously positioned for some participants. In these cases, participants were contacted and rescanned on a separate day where possible. However, where rescanning was not possible, the visual cortex data for these participants were excluded.

In total, one participant was excluded from the right basal ganglia analysis: 1 SZ (data quality). Furthermore, 10 participants were excluded for visual NAA concentrations: 1 HC

(voxel placement), 7 REL (6 for voxel placement; 1 for data quality) and 2 SZ (voxel placement). The number of participants that were included for each group and voxel placement is described in table 3 and the total number of participants with both useable DTI and MRS data is presented in table 4.

***Tissue Segmentation***

3T anatomical scans were co-registered to the 7T anatomical scan for each respective participant and subsequently segmented using the unified segmentation method (Ashburner & Friston, 2005) into gray matter, white matter, and cerebrospinal fluid probability maps. Binary masks for each MRS voxel were generated. For each of the three tissue masks in the visual cortex, MRS voxel values were summed together and divided by the sum of voxel values of each tissue mask within the MRS location. Thus, our calculated fraction of gray matter ($f_{GM}$), fraction of white matter ($f_{WM}$) and fraction of CSF ($f_{csf}$) were such that $f_{GM} + f_{WM} + f_{CSF} = 1$.

Our procedure for tissue segmentation in the basal ganglia differed because automated segmentation of subcortical regions can be less accurate than in the cortex. For the basal ganglia, we normalized 20 high-resolution T1 scans from healthy controls into the standard MNI space using the unified segmentation method. These scans were then averaged together which produced a map in which basal ganglia structures were more visible than in any of the individual anatomical scans. A normalized basal ganglia mask was created by manually delineating the caudate, putamen and globus pallidus on this averaged scan. For each participant, the basal ganglia mask was then warped back into native space using inverse normalization parameters obtained during segmentation. For the basal ganglia MRS location, the GM mask was defined as the union of the basal ganglia mask and the probabilistic GM mask obtained using the automated segmentation procedure. Fractions of gray matter, white matter and cerebrospinal fluid were the

calculated using the procedure described above. Finally, the proportion of the measurement voxel which was comprised by the basal ganglia mask was calculated.

***Partial Volume Correction***

Fractions of gray matter (both total and basal ganglia only for the subcortical voxel), white matter, and cerebrospinal fluid were obtained via segmentation of T1-weighted anatomic images obtained at 3T. The ratio of the area under the NAA peak to the area under the water peak was corrected for partial volume effects of gray matter, white matter and cerebrospinal fluid using the following equations:

**[Eq. 1]**

$$Corr_{NAA} = \frac{Area_{NAA}}{Area_{water}} x \frac{(WConc_{gm} x Att_{water\_GM}) + (Wconc_{WM} x Att_{water\_WM}) + (WConc_{CSF} x Att_{Water\_CSF})}{(1 - F_{CSF}) x ATT_{NAA}}$$

In which $Att_{water\_T}$ is the relaxation attenuation factor of water in each type of tissue (GM, WM & CSF) respectively. $Att_{water\_T}$ was calculated using the following equation:

**[Eq. 2]**

$$Att_{water\_T} = \exp\left(-\frac{TE}{T_{2_{water_t}}}\right) x \left(1 - \exp\left(-\frac{TR}{T_{1_{water_t}}}\right)\right)$$

In eq. 2, TR is the repetition time and TE is the sequence echo time. $T_{1_{water_t}}$ and $T_{2_{water_t}}$ are based on values reported by Marjańska et al. (2012). In eq. 1, $ATT_{NAA}$ was the relaxation factor of the metabolite, n-acetylaspartate. It was assumed to be the same in GM and WM and was calculated using the following equation:

**[Eq. 3]**

$$ATT_{NAA} = \exp(-\frac{TE}{T_{2_{NAA}}})$$

TE is the sequence echo time and $T_{2_{NAA}}$ is based on values reported in Marjanska et al. (2013) as presented in table 5.

Finally, $WConc_t$ in Eq. 1 refers to the NMR-visible water concentration (mM) in gray matter, white matter, and cerebrospinal fluid, respectively. $WConc_t$ was calculated using the formula:

**[Eq. 4]**

$$WConc_t = f_t x WD_t$$

Where $f_t$ is the tissue volume fractions obtained by tissue segmentation and $WD_t$ is the density of water in each tissue type. This was obtained by multiplying pure water density (55556 mM) by the proportion of water in each type of tissue (gray matter: 0.78, white matter: 0.65, cerebrospinal fluid: 0.97) as reported by (Ernst et al., 1993).

***Statistical Analyses***

Statistical analyses were performed in R studio and SPSS. ANOVA and Chi-square tests were used to compare demographics. For both the visual cortex and basal ganglia voxel, one-way ANCOVA were used to compare NAA concentrations across groups while controlling for age and proportion of gray matter present in the respective voxel. Due to heterogeneity of error variance, NAA concentrations were transformed using the natural logarithm (ln) before analyses. Posthoc analyses were conducted using a Bonferroni correction for multiple comparisons. To explore the relationship between NAA concentrations and symptoms in SZ, partial correlations were computed between NAA concentration in both voxels and PANSS positive, PANSS

negative and PANSS total scores, controlling for age and proportion of gray matter in the respective voxel.

**Diffusion Tensor Imaging**

***Image acquisition***

DTI data were acquired at the University Medical Center on an Achieva 3T scanner equipped with an eight-channel head coil allowing parallel imaging. Two diffusion images were acquired using single-shot echoplanar imaging sequences, consisting of 30 diffusion-weighted scans (b  1000 s/mm2) with noncollinear gradient directions and one image without diffusion weighting (b  0 s/mm2), covering the entire brain [repetition time (TR)  7057 ms; echo time (TE) 68 ms; field of view  240 x 240 x150 mm; in-plane resolution  1.875  1.875 mm; slice thickness 2 mm; no slice gap; 75 axial slices; matrix size, 128 x 99 mm]. The diffusion-weighted scans were measured twice, once with phase encoding direction reversed (first scan, posterior—anterior; second scan, anterior–posterior), to correct for susceptibility-induced spatial distortions (Andersson and Skare, 2002). For registration purposes, a whole brain three-dimensional T1-weighted scan (200 slices; TR  10 ms; TE 4.6 ms; flip angle 8°; field of view, 240 x 240 x 160 mm; voxel size: 0.75 x 0.8 x 0.75 mm) was acquired.

***Preprocessing***

DTI scans were visually examined for image quality then preprocessed and analyzed using FSL 5.0 (FMRIB Software Library; www.fmrib.ox.ac.uk/ fsl) to correct for the effects of eddy-currents. This procedure is outlined in (Yao et al., 2020) but briefly: diffusion data were acquired using reverse phase-encoding blips which resulted in pairs of images with distortions in opposite directions. Using these pairs of images, the off-resonance field was estimated using a technique similar to that outlined by (Andersson & Skare, 2002) and (Smith et al., 2004). Using

default affine registration procedures, we realigned the diffusion weighted imaged from each phase-encoding direction to the b0 image. Finally, we used the default settings on the *eddy_correct* command to correct for subject movements and eddy current induced distortions. Eddy-corrected scans with opposite phase-encoding blips were then combined into a single corrected image with the applytopup command. The mean b0 image was used to create a brain mask which was then applied to all diffusion-weighted images.

Diffusion data was fitted to a tensor model using the DTIFIT command in the FMRIB library which resulted in the calculation of three eigenvalues at each voxel (λ1, λ2, λ3). These values were used to calculate a fractional anisotropy (FA), radial diffusivity (RD), axial diffusivity (AD) and mean diffusivity (MD) value at each voxel using the following formula (Pierpaoli & Basser (1996); see Alexander, Lee, Lazar & Field (2007) for a review of DTI metrics):

$$\text{FA} = \sqrt{\frac{(\lambda 1 - \lambda 2)^2 + (\lambda 2 - \lambda 3)^2 + (\lambda 1 - \lambda 3)^2}{2(\lambda 1^2 + \lambda 2^2 + \lambda 3^2)}}$$

$$\text{RD} = \frac{(\lambda 2 + \lambda 3)}{2}$$

$$\text{AD} = \lambda_1$$

$$\text{MD} = \frac{(\lambda 1 + \lambda 2 + \lambda 3)}{3}$$

***Diffusivity measures of microstructural integrity***

Fractional anisotropy is a common measure of white matter microstructural integrity. FA measures the extent to which diffusion along a tract is uniform (that is occurring in the same direction). FA ranges from 0 (isotropic) to 1 (anisotropic) where higher FA values represent stronger degrees of directionality, thus inferring better microstructural integrity. Although the interpretation of fractional anisotropy is controversial, data suggests that FA can be an accurate

measure of white matter structure and is particularly sensitive to detecting fiber coherence (Choi et al., 2015). However, whilst FA may provide knowledge about general structural changes in WM, FA does not provide information about the causes of these changes. For example, reduced FA could reflect either myelin or axonal damage. MD is a non-specific measure of white matter microstructure. It is believed to be an inverse measure of membrane density such that lower MD represents higher anisotropy in tissue. MD values have been shown to negatively correlate with diffusion-restricting materials such as myelin (Seehaus et al., 2015) as well as cell and axonal density (Stolp et al., 2018).

Given that FA and MD are general measures of diffusion, RD and AD values can also be examined to understand specific changes in microstructure. RD measures the magnitude to which water diffuses perpendicular to the principal diffusion direction. RD has been shown to correlate strongly with both myelin density and fiber coherence (Choi et al., 2015; Song et al., 2002), which suggests that RD may be a more sensitive measure of demyelination where lower RD reflects higher degrees of myelination in a region. AD measures the magnitude to which water diffusion occurs parallel to the principal diffusion direction. AD has been shown to correlate with axonal damage (Budde et al., 2009) and injury (Aung et al., 2013) such that reduced AD reflects higher degrees of axonal damage.

***Voxel-based Analysis Using Tract-Based Spatial Statistics***

All four diffusion measures (FA, RD, MD, and AD) were compared across groups and related to NAA using tract-based spatial statistics (TBSS; Smith et al., 2006). TBSS is a procedure in FSL (Smith et al., 2004) where each participant's diffusivity data (FA, RD, MD and AD) is projected onto a mean FA skeleton before applying cross-subject, voxelwise statistics. First, FA images were created by fitting tensor models to the raw diffusion data using FDT and

brain-extracted using BET (Smith, 2002). Next, we used the nonlinear registration tool FNIRT to align each subjects' FA data into a common (MNI) space (Andersson, 2007a; Andersson, 2007b). These images were then combined to create a mean FA image which was thinned to produce a FA skeleton representing the major white matter tracts of the study's subjects. Finally, each subject's aligned diffusivity data were then projected onto this white matter skeleton and the resulting data were analyzed using voxelwise statistics.

Group differences in FA, MD, AD and RD were compared at each voxel within this white matter skeleton using FSL's randomize function with 10,000 permutations and 2mm variance smoothing, while controlling for participant age and proportion of gray matter within the MRS voxel. Threshold-Free Cluster Enhancement was used to correct for multiple comparisons and a corrected p-value of 0.05 was adopted for all analyses (Winkler et al., 2014). ANCOVA was conducted at each voxel using the randomize function to correlate NAA concentrations with DTI measures whilst controlling for age and the proportion of gray matter within the MRS voxel. FSL's cluster command was used to identify inferential statistic values, cluster sizes and MNI coordinates for clusters of significance. Anatomical locations of clusters were derived from the Johns Hopkins White Matter Labels atlas (Mori et al, 2008; Oishi et al, 2008). Data was visualized using the TBSS_Fill and FSLeyes commands.

## RESULTS

### Group differences in NAA concentrations

Reported means and SD are estimated marginal means unless otherwise stated. There was a significant group difference in the concentrations of NAA in the visual cortex when controlling for age and the proportion of gray matter (Fig. 3; $F(2, 53) = 7.304$, $p = 0.002$, partial $\eta^2 = 0.216$). Post-hoc analyses revealed that SZ had significantly lower NAA concentrations (mean = 8.081, SD = 0.93) than HC (mean = 9.205, SD = 0.87, $p < 0.001$). NAA concentrations of REL (mean = 8.687, SD = 0.92) did not differ from either SZ ($p = 2.07$) or HC ($p = 0.257$; figure 3).

We found no group differences in NAA concentrations in the right basal ganglia ($F(2, 62) = 1.122$, $p = 0.332$, partial $\eta^2 = 0.035$; figure 4).

### NAA concentration and symptoms

A partial correlation analysis was used to determine the relationship between NAA concentration and symptom scale scores whilst controlling for age and % of gray matter in the voxel. There was no association between visual cortex NAA and scores on the PANSS positive ($r(15) = -0.262$, $p = 0.310$), negative ($r(15) = 0.086$, $p = 0.744$) and general scales ($r(15) = -0.191$, $p = 0.463$). Similarly, there was no significant association between NAA concentrations in the right basal ganglia and PANSS positive ($r(16) = -0.205$, $p = 0.414$), negative ($r(16) = -0.132$, $p = 0.602$) and general ($r(16) = -0.110$, $p = 0.663$) scores.

### TBSS-Group differences

There were no group differences in FA, RD, AD or MD when controlling for age that survived multiple comparison corrections.

**TBSS – Correlations with NAA concentrations**

***Visual Cortex NAA***

**Fractional Anisotropy**. There was no significant relationship between concentrations of NAA in the visual cortex and fractional anisotropy.

**Mean Diffusivity.** There was a significant, sample wide effect of NAA on MD such that lower concentrations of NAA predicted higher mean diffusivity in the right superior longitudinal fasciculus, anterior thalamic radiation, and forceps minor (figure 5; table 6). We found no group-by-NAA effect suggesting that the relationship between NAA and MD did not differ between groups.

**Radial Diffusivity.** There was a significant, sample wide effect of NAA on RD in parts of the superior longitudinal fasciculus whereby lower concentrations of NAA predicted higher RD (figure 6; table 6). We found no group-by-NAA effect suggesting that the relationship between NAA and RD did not differ between groups.

**Axial diffusivity.** There was a sample-wide, significant effect of NAA concentration on axial diffusivity such that lower NAA concentration predicted higher AD in the right anterior thalamic radiation, forceps minor and the right superior longitudinal fasciculus (figure 7; table 6). We found no group-by-NAA effect suggesting that the relationship between NAA and AD did not differ between groups.

***Basal Ganglia NAA***

**Fractional Anisotropy**. We found a significant sample-wide positive relationship between NAA concentrations in the basal ganglia and FA in the right inferior front-occipital fasciculus, right anterior thalamic radiation, and the right superior longitudinal fasciculus (figure 8; table 7). Increased concentrations of NAA in the right basal ganglia correlated with increased

FA in these regions. We found no group-by-NAA effect suggesting that the relationship between NAA and FA did not differ between groups.

**Mean diffusivity.** There was no significant effect of NAA concentrations in the basal ganglia and mean diffusivity.

**Radial diffusivity.** NAA concentrations in the right basal ganglia had a significant effect on radial diffusivity in the forceps minor and the left anterior thalamic radiation (figure 9; table 7), such that lower NAA concentrations correlated with higher radial diffusivity. We found no group-by-NAA effect suggesting that the relationship between NAA and RD did not differ between groups.

**Axial diffusivity**. NAA concentrations in the basal ganglia had a significant effect on axial diffusivity in the left anterior thalamic radiation across our entire sample (figure 10; table 7). Lower basal ganglia NAA predicted elevated axial diffusivity in this region. We found no group-by-NAA effect suggesting that the relationship between NAA and AD did not differ between groups.

## DISCUSSION

We used a combination DTI-MRS approach to study the relationship between concentrations of NAA in the basal ganglia and visual cortex, and the structural integrity of white matter in a sample of persons with schizophrenia, unaffected first-degree relatives, and healthy controls. We predicted that persons with schizophrenia and their relatives would have reduced concentrations of NAA compared to healthy controls, and that these reduced NAA concentrations would correlate with diffusivity measures in white matter. In persons with schizophrenia, but not relatives, we found significant reductions in visual cortex NAA compared to controls. Although there was no effect of group on diffusivity measures, NAA concentrations in the visual cortex and basal ganglia correlated with diffusivity measures that were generally consistent with poor white matter microstructure. These findings add to a growing literature which suggests that NAA may contribute to white matter abnormalities in schizophrenia (Reid et al., 2016; Tang et al., 2007) and will be discussed in more detail below.

Consistent with previous literature, we observed significant reductions in NAA concentrations of persons with schizophrenia compared to healthy controls (Iwata et al., 2018; Kraguljac et al., 2012). As NAA has well-documented roles in the synthesis and production of myelin (Chakraborty et al., 2001; D'Adamo & Yatsu, 1966), our finding of reduced visual cortex NAA in persons with schizophrenia provides preliminary support for the hypothesis that reduced availability of NAA may contribute to white matter abnormalities in schizophrenia through preventing the generation, and repair, of myelin.

However, whilst our findings are in-line with research reporting broad reductions of NAA in persons with schizophrenia, they stand in contrast to the results of meta-analyses which have concluded that visual cortex NAA is not reduced in schizophrenia (Steen et al., 2005;

Whitehurst et al., 2020). Steen et al. (2005) analyzed studies measuring both NAA and NAA/Cr whereas Whitehurst et al. (2020) focused their analysis on those papers which calculated NAA with respect to water. Thus, the meta-analytic findings of Whitehurst et al. (2020) are most relevant to our study. Of particular interest, Whitehurst et al. (2020) determined that their analysis was underpowered for detecting group differences in visual cortex NAA; a finding which is corroborated by other authors who have suggested that the current evidence against reduced VC NAA in schizophrenia is of low-to-moderate quality (Tohid et al., 2015). Thus, the contradiction of previous literature with our current findings may be the consequence of a dearth of studies investigating visual cortex NAA concentrations in schizophrenia, suggesting this may be an area for additional study, especially given the prevalence of visual distortions in persons with schizophrenia (Gracitelli et al., 2015).

That we did not find a significant difference in the concentration of basal ganglia NAA is consistent with previous meta-analyses (Steen et al., 2005; Whitehurst et al., 2020). Given that observations of reduced NAA tend to occur in brain regions where reductions in tissue volume are also evident (Steen et al., 2005), the lack of significant difference in basal ganglia NAA is not surprising because basal ganglia volumes in persons with schizophrenia tend to be enhanced when compared to healthy controls (Shenton et al., 2001).

There was no significant difference in the NAA concentrations of first-degree relatives when compared to persons with schizophrenia or healthy controls. Whilst meta-analyses have consistently reported evidence of reduced NAA concentration in first-degree relatives (Brugger et al., 2011; Mondino et al., 2013), these reductions appear to be region specific. Basal ganglia NAA concentrations do not appear to differ between first-degree relatives, persons with schizophrenia and healthy controls (Brugger et al., 2011), which is consistent with the findings

of the present study. Furthermore, research examining concentrations of NAA in the visual cortex of first-degree relatives appears scarce with Brugger et al. (2011) failing to identify a single study that had examined visual cortex NAA in first-degree relatives. Despite not reaching statistical significant, there was a medium effect size of difference between visual cortex NAA concentrations of relatives and healthy controls, and relatives and persons with schizophrenia. Given our small sample sizes, the lack of significant differences in visual cortex NAA concentrations of relatives may be related to lack of power. Thus, this pattern of differences in NAA concentrations may reflect a general vulnerability towards psychosis in which greater reductions of NAA reflect greater risk of developing the illness. However, because relatives did not differ from persons with schizophrenia, or healthy controls, we are unable to conclude whether or not reductions in NAA in individuals with schizophrenia may reflect a proximal illness mechanism or general vulnerability towards schizophrenia. Future studies should try to replicate our findings using a larger sample of first-degree relatives.

Across groups, we found correlations between both visual cortex and basal ganglia NAA concentrations and diffusivity in white matter tracts which connect the frontal-, occipital-, parietal- and temporal regions. Lower NAA concentrations in the visual cortex predicted higher MD, RD, and AD values. Likewise, lower NAA concentrations in the basal ganglia predicted lower FA and higher RD and AD values. These results broadly indicate that reduced NAA concentrations are associated with poorer measures of white matter integrity. More specifically, lower concentrations of NAA appear to correlate with increased diffusion of water in tissues (MD) and less uniform diffusion directions (FA). While MD is an aspecific marker of white matter integrity, accumulating evidence suggests that both decreased FA and increased RD correlate with demyelination in both animal (Budde et al., 2011; Song et al., 2003; Sun et al.,

2006) and human (Kronlage et al., 2017) samples whereas reduced AD typically correlates with axonal damage (Song et al., 2003; Sun et al., 2006). That both increased MD, and decreased FA, occurred alongside elevated RD values in our sample suggests that demyelination is contributing to these abnormal patterns of diffusion.

Interestingly, we found that AD was increased in the presence of reduced NAA. Our observed negative correlations between NAA concentration and AD are consistent with previous research which has also reported inverse relationships between NAA concentrations and AD in schizophrenia (Reid et al., 2016), individuals with white matter diseases (Hannoun et al., 2012) and healthy controls (Ghosh et al., 2017). Whilst inverse relationships between NAA and AD appear robust, they may be surprising considering that AD is often reported to be a measure of axonal damage (Song et al., 2003; Sun et al., 2006), thus suggesting that reduced NAA is related to less axonal damage. However, increased AD can occur in the presence of increased RD (Bennett et al., 2010; Della Nave et al., 2011; Hope et al., 2019) with researchers suggesting that higher AD values may reflect the increased axonal space which occurs as a result of demyelination (Rosas et al., 2010). Combined, the pattern of our data lends preliminary support to the argument that reduced NAA concentrations may contribute to the white matter abnormalities observed in clinical populations through its effects on myelination.

However, our pattern of results could be explained by alternative hypotheses. For example, evidence suggests that NAA can facilitate energy production through promoting an alternative pathway for the conversion of glutamate to α-ketoglutarate in mitochondria (Moffett et al., 2013). Indeed, research has demonstrated that ATP synthesis and NAA synthesis are coupled (Patel & Clark, 1979) such that lower ATP predicts lower NAA synthesis and NAA concentrations have been shown to decrease dramatically in the presence of energy impairment

caused by traumatic brain injury (Signoretti et al., 2001); a reduction which is permanent in cases of severe mitochondrial dysfunction (Di Pietro et al., 2014). Thus, our results could also be interpreted in terms of the bioenergetic properties of NAA whereby reduced availability of NAA results in mitochondria resorting to the glutamate dehydrogenase reaction to generate α-ketoglutarate which produces ammonia as a biproduct. Increased reliance on this reaction would result in increasingly neurotoxic levels of ammonia in the brain (Moffet et al., 2013), thus leading to gradual degradations of white matter. Such an observation is supported by our observed negative correlations between NAA and MD & RD.

While our research design does not allow us to differentiate between these two hypotheses, it is likely that the observed correlations between concentrations of NAA and diffusivity measures reflect a combination of NAA's involvement in myelin synthesis and energy production. Indeed, degradations in white matter caused by reduced NAA availability are likely to exacerbate the energy demands placed upon mitochondria, as accumulating evidence suggests that mitochondria may compensate for the increased energy demands of an axon following myelin injury (Campbell & Mahad, 2011). Thus, these complimentary functions may explain the gradual white matter degradations observed in persons with schizophrenia (Cropley et al., 2017) and would generally be supported by our observations of reduced NAA concentration in persons with schizophrenia and the correlations between white matter diffusivity and NAA concentrations. Future research could begin to differentiate between these explanations by measuring white matter integrity with more specific imagining techniques (e.g. T2 relaxation) which would allow researchers to directly measure myelination in vivo.

Our results appear to lend limited support to the dysconnection hypothesis (Stephan et al., 2009). Consistent with our hypotheses, we found significantly reduced concentrations of NAA in

persons with schizophrenia. Furthermore, NAA concentrations were found to correlate with measures of white matter integrity. However, despite significantly reduced visual cortex NAA, the correlations between NAA concentration and our DTI measures were not specific to persons with schizophrenia. Whilst this pattern of results is consistent with previous MRS-DTI studies (Chiappelli et al., 2015; Tang et al., 2007), the lack of group differences in white matter diffusivity in our sample suggests that differences in NAA concentration cannot solely account for white matter abnormalities in persons with schizophrenia.

The lack of group differences in diffusivity measures is surprising given the number of studies that have reported differences in diffusion metrics between persons with schizophrenia and healthy controls (Ellison-Wright & Bullmore, 2010; Kelly et al., 2018). However, these differences are often small. For example, in a large multi-site DTI analysis, Kelly et al. (2018) reported differences in FA between healthy controls and individuals with schizophrenia with effect sizes that ranged between 0.1 and 0.4. Given these small effect sizes, it is possible that the lack of group differences in the current analysis is a result of our study being underpowered. Indeed, the inclusion of first-degree relatives could have further compounded this issue as their diffusion measures tend to be between those of healthy controls and persons with schizophrenia (Prasad et al., 2015) which may have diluted any group effects. Thus, our sample might have been too small to detect these subtle group effects.

In additional to a relatively small sample size, our study is subject to several other limitations. Firstly, our clinical sample was relatively high functioning with mild symptoms as evidenced by their low PANSS scores (Table 1 & Tables 2). Thus, our sample may not represent a typical sample of persons with schizophrenia. This could also explain why we failed to replicate previous findings of white matter differences in persons with schizophrenia as emerging

evidence suggests that fractional anisotropy may correlate with symptom severity (Yang et al., 2017). An additional limitation is that we included a fully medicated sample, so we cannot rule out any confounding effects of medication. Thus, whilst inclusion of first-degree relatives allows us to infer that reductions in NAA may not be a putative illness marker, we cannot determine whether the reduced visual cortex NAA in persons with schizophrenia is a result of the illness or long-term medication use. However, recent research has suggested that long-term antipsychotic use does not affect concentrations of NAA (Grošić et al., 2014).

Despite these limitations, the results of this study add to a growing literature and interest in the relationship between NAA and white matter in schizophrenia. Although MRS and DTI studies are common in schizophrenia research, their joint application represents an opportunity to better understand the neural mechanisms implicated in schizophrenia. Future studies should examine the relationship between concentrations of NAA and white matter using more targeted imaging techniques with a larger sample. The current literature would also benefit from a prospective MRS-DTI approach in which the NAA concentrations and white matter integrity of persons with schizophrenia are followed over time, thus allowing us to examine whether reductions in NAA precede or follow differences in myelination.

To conclude, we used a joint MRS-DTI approach to explore the relationship between concentrations of NAA and white matter integrity in persons with schizophrenia, first-degree relatives, and healthy controls. We used 7T MRS to quantify concentrations of NAA with respect to water and found a significant reduction in NAA concentration in the visual cortex of persons with schizophrenia. Although we found no group differences in DTI measures, we found overall correlations between diffusivity measures in major white matter tracts and NAA concentrations in the basal ganglia and visual cortex. Taken together, our results suggest that the concentrations

of NAA appear to be related to the integrity of white matter. These results demonstrate the utility of combined MRS-imaging approaches to understanding the causes of white matter changes in schizophrenia. Future studies should seek to build on these findings by using more specific imagining techniques in a larger sample to understand how NAA concentrations may affect white matter microstructure.

# APPENDICES

# APPENDIX A

## Tables

**Table 1.**

Demographic info for individuals with MRS data

| | **Healthy Controls (n = 24)** | **Relatives (n = 23)** | **Persons with SZ (n = 21)** | **Statistics** | ***p-value*** |
|---|---|---|---|---|---|
| Age | 33.92 (9.28) | 31.22 (5.44)* | 36.43 (7.29) | *Welch's F* = 3.601 | 0.036 |
| Sex (female/male) | 8/16 | 8/15 | 6/15 | $\chi^2 = 38.114$ | 0.900 |
| Education[a] | 7.37 (1.06) | 6.39 (1.67) | 4.71 (1.82) | $\chi^2 = 37.579$ | P < 0.001 |
| Handedness[b] | 0.76 (0.57) | 0.87 (0.29) | 0.94 (0.19) | *Welch's F = 1.293* | 0.286 |
| Smoking (non-smoker/smoker) | 18/3 | 16/7 | 12/6 | $\chi^2 = 2.246$ | 0.325 |
| NVIQ | 100.57 (13.02) | 101.22 (14.04) | 95.86 (12.70) | *F* = 1.040 | 0.359 |
| Illness Duration | | | 14.00 (4.24) | | |
| PANSS Pos | | | 11.38 (4.66) | | |
| PANSS Neg | | | 12.38 (5.52) | | |
| PANSS Gen | | | 25.00 (7.38) | | |
| CPZ equivalent Dose | | | 282.89 (241.75) | | |

Notes: Values are presented as mean (SD)

* Indicates sig. difference in vs SZ group

a. Education categories: 0 = less than 6 years of primary education; 1 = finished 6 years of primary education; 2 = 6 years of primary education and low-level secondary education; 3 = 4 years of low-level secondary education; 4 = 4 years of average-level secondary education; 5 = 5 years of average-level secondary education; 6 = 4 years of secondary vocational training; 7 = 4 years of high-level professional education; 8 = university degree.

b. Based on the Edinburgh Handedness Inventory; scores range from -1 indicating complete left-handedness to 1 indicating complete right-handedness

**Table 2.**

Demographic data for individuals with DTI data

| | **Healthy Controls (n = 44)** | **Relatives (n = 20)** | **Persons with SZ (n = 22)** | **Statistics** | ***p-value*** |
|---|---|---|---|---|---|
| Age | 30.3 (8.4)* | 31.7 (5.6)* | 37.4 (7.8) | *F = 6.37* | 0.003 |
| Sex (female/male) | 22/22 | 7/13 | 5/17 | $\chi^2 = 4.79$ | 0.09 |
| Education[a] | 7.0 (1.4) | 6.4 (1.8) | 4.8 (1.7) | $\chi^2 = 33.78$ | P < 0.001 |
| Handedness[b] | 0.71 (0.65) | 0.88 (0.30) | 0.85(0.45) | *F = 0.95* | 0.39 |
| Smoking (non-smoker/smoker) | 42/2 | 13/7 | 14/8 | $\chi^2 = 13.175$ | P < 0.001 |
| NVIQ | 100.2 (12.0) | 104.2 (12.2) | 96.0 (12.8) | *F = 2.38* | 0.10 |
| Illness Duration | | | 14.2 (5.2) | | |
| PANSS Pos | | | 11.6 (5.2) | | |
| PANSS Neg | | | 13.1 (6.3) | | |
| PANSS Gen | | | 25.0 (7.9) | | |
| CPZ equivalent Dose | | | 281.3 (249.6) | | |

*Notes*: Values are presented as mean (SD)

***** Indicates sig. difference in vs SZ group

a. Education categories: 0 = less than 6 years of primary education; 1 = finished 6 years of primary education; 2 = 6 years of primary education and low-level secondary education; 3 = 4 years of low-level secondary education; 4 = 4 years of average-level secondary education; 5 = 5 years of average-level secondary education; 6 = 4 years of secondary vocational training; 7 = 4 years of high-level professional education; 8 = university degree.

b. Based on the Edinburgh Handedness Inventory; scores range from -1 indicating complete left-handedness to 1 indicating complete right-handedness.

**Table 3.**

Total number of participants with useable spectra for each voxel location

| | HC | REL | SZ | Total |
|---|---|---|---|---|
| **Visual Cortex** | 23 | 16 | 19 | 58 |
| **Right Basal Ganglia** | 24 | 23 | 20 | 67 |

**Table 4.**

Total number of participants with both useable DTI and MRS data

| | **HC** | ***REL*** | ***SZ*** | ***Total*** |
|---|---|---|---|---|
| ***Visual Cortex*** | *19* | *13* | *18* | *50* |
| ***Right Basal Ganglia*** | *18* | *20* | *19* | *57* |

**Table 5.**

$T_2$ values for Visual Cortex and Basal Ganglia NAA as reported by Marjanska et al. (2013)

| | $T_{2_{NAA}}\ (ms)$ |
|---|---|
| Visual Cortex NAA | 132 |
| Basal Ganglia NAA | 130 |

**Table 6.**

Clusters showing significant correlations between DTI measurements and NAA measured in the visual cortex

| | MNI Coordinates | | | Cluster Size | t | p-corrected |
|---|---|---|---|---|---|---|
| | X | Y | Z | | | |
| **Negative Correlation: RD** | | | | | | |
| Superior Longitudinal Fasciculus | -12 | 17 | 30 | 1484 | 5.33 | 0.049 |
| **Negative Correlation: MD** | | | | | | |
| Forceps minor | 17 | 34 | 7 | 4451 | 4.43 | 0.036 |
| Superior Longitudinal Fasicuclus | 32 | -27 | 39 | 2873 | 5.07 | 0.032 |
| **Negative Correlation: AD** | | | | | | |
| Forceps Minor | 21 | 35 | 9 | 439 | 4.45 | 0.039 |
| Superior longitudinal fasciculus | 32 | -25 | 39 | 210 | 4.07 | 0.046 |

*Notes*: *structures identified refer to the peak for each voxel cluster as identified by the JHU White-Matter Tractography Atlas*

**Table 7.**

Clusters showing significant correlations between DTI measurements and NAA measured in the right basal ganglia

| | MNI Coordinates | | | Cluster Size | *t* | *p-corrected* |
|---|---|---|---|---|---|---|
| | X | Y | Z | | | |
| **Entire Sample** | | | | | | |
| **Negative Correlation: RD** | | | | | | |
| Anterior Thalamic Radiation | -21 | 33 | 14 | 639 | | 0.046 |
| **Negative Correlation: AD** | | | | | | |
| Anterior Thalamic Radiation | -6 | -20 | 14 | 48 | | 0.037 |
| **Positive Correlation: FA** | | | | | | |
| Inferior fronto-occipital fasciculus | -24 | 35 | 1 | 6848 | | 0.001 |
| Inferior Fronto-occipital fasciculus | 33 | 35 | 0 | 1642 | | 0.049 |
| Superior longitudinal fasciculus | 44 | -45 | 6 | 304 | | 0.041 |

Notes: structures identified refer to peak of each voxel cluster as identified by the JHU White-Matter Tractography Atlas

# APPENDIX B

## Figures

**Figure 1.**

Voxel placement for T1 anatomical weighted scans.

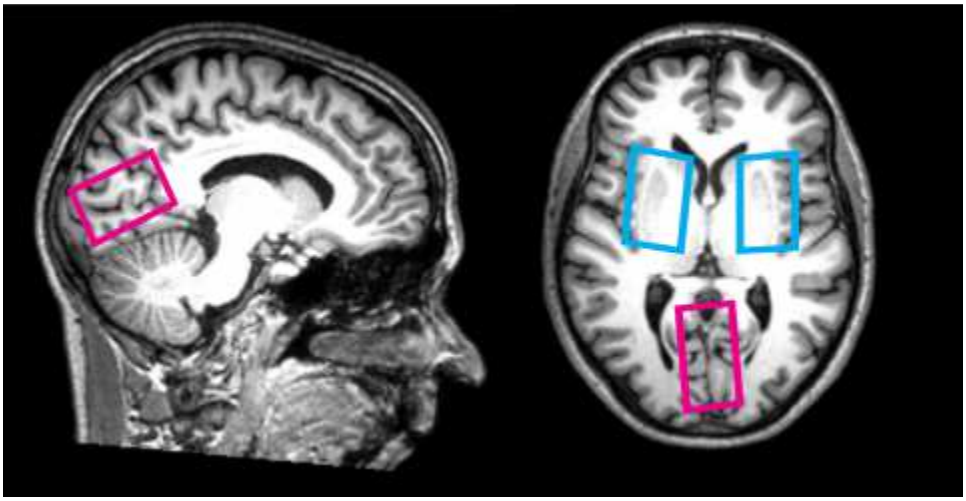

*Note.* Voxel placement for T1 scans on a representative participant for visual cortex (magenta) and basal ganglia voxels. Basal ganglia voxels were positioned to include as much striatum as possible. The visual cortex voxel was positioned symmetrically around the calcarine sulcus and included both left and right hemispheres. Reprinted from "7T Proton Magnetic Resonance Spectroscopy of Gamma-Aminobutyric Acid, Glutamate, and Glutamine Reveals Altered Concentrations in Patients With Schizophrenia and Healthy Siblings" by K.N. Thakkar et al, 2017, *Biological Psychiatry, 81, p. 527.* Copyright 2010 by Elsevier.

**Figure 2.**

Representative spectra fits (black) and raw data fits (blue) from Proton Magnetic Spectroscopy in the Visual Cortex (left) and Basal Ganglia (right) from a single subject.

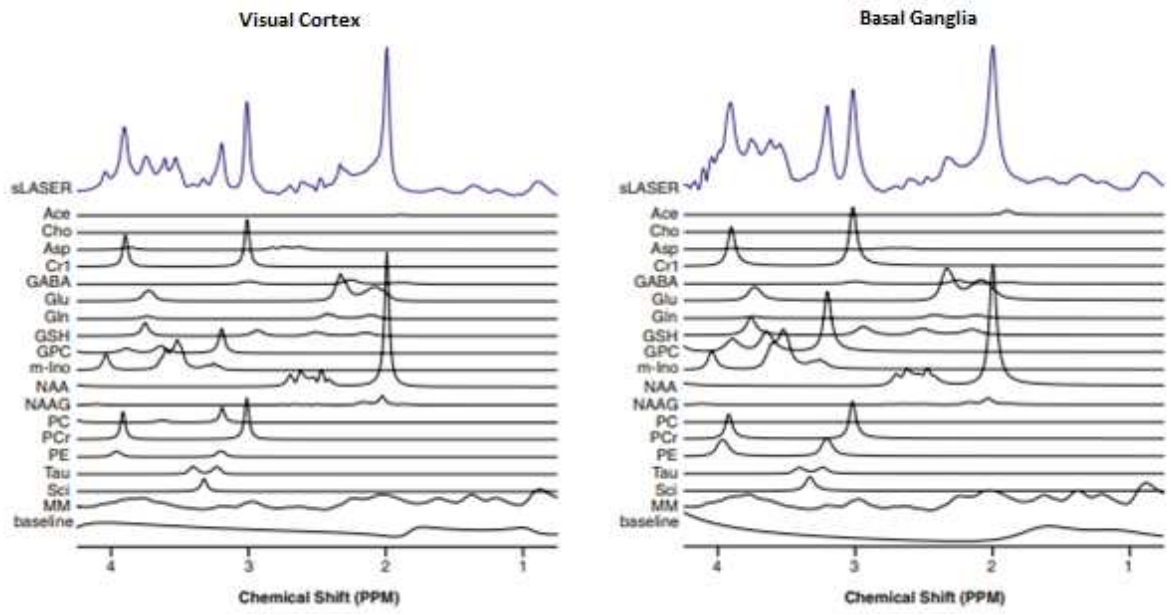


*Note*. Baseline includes signal contributions of water and lipids. Ace, acetate; Asp, aspartate; Cho, choline; Cr1, creatine; GABA, gamma-aminobutyric acid; Gln, glutamine; Glu, glutamate; GPC, glycerophosphorylcholine; GSH, glutathione; m-Ino, myo-inositol; MM baseline, macromolecule baseline; NAA, N-acetylaspartate; NAAG, N-acetylaspartylglutamate; PC, phosphocholine; PCr, phosphocreatine; PE, phosphoethanolamine; PPM, parts per million; Sci, scyllo-inositol; sLASER, semilocalized by adiabatic selective refocusing (sequence); Tau, taurine. Reprinted from "7T Proton Magnetic Resonance Spectroscopy of Gamma-Aminobutyric Acid, Glutamate, and Glutamine Reveals Altered Concentrations in Patients With Schizophrenia and Healthy Siblings" by K.N. Thakkar et al, 2017, *Biological Psychiatry*, 81, p. 527. Copyright 2010 by Elsevier.

**Figure 3.**

Estimated concentrations of NAA in the visual cortex when controlling for age and % of gray matter.

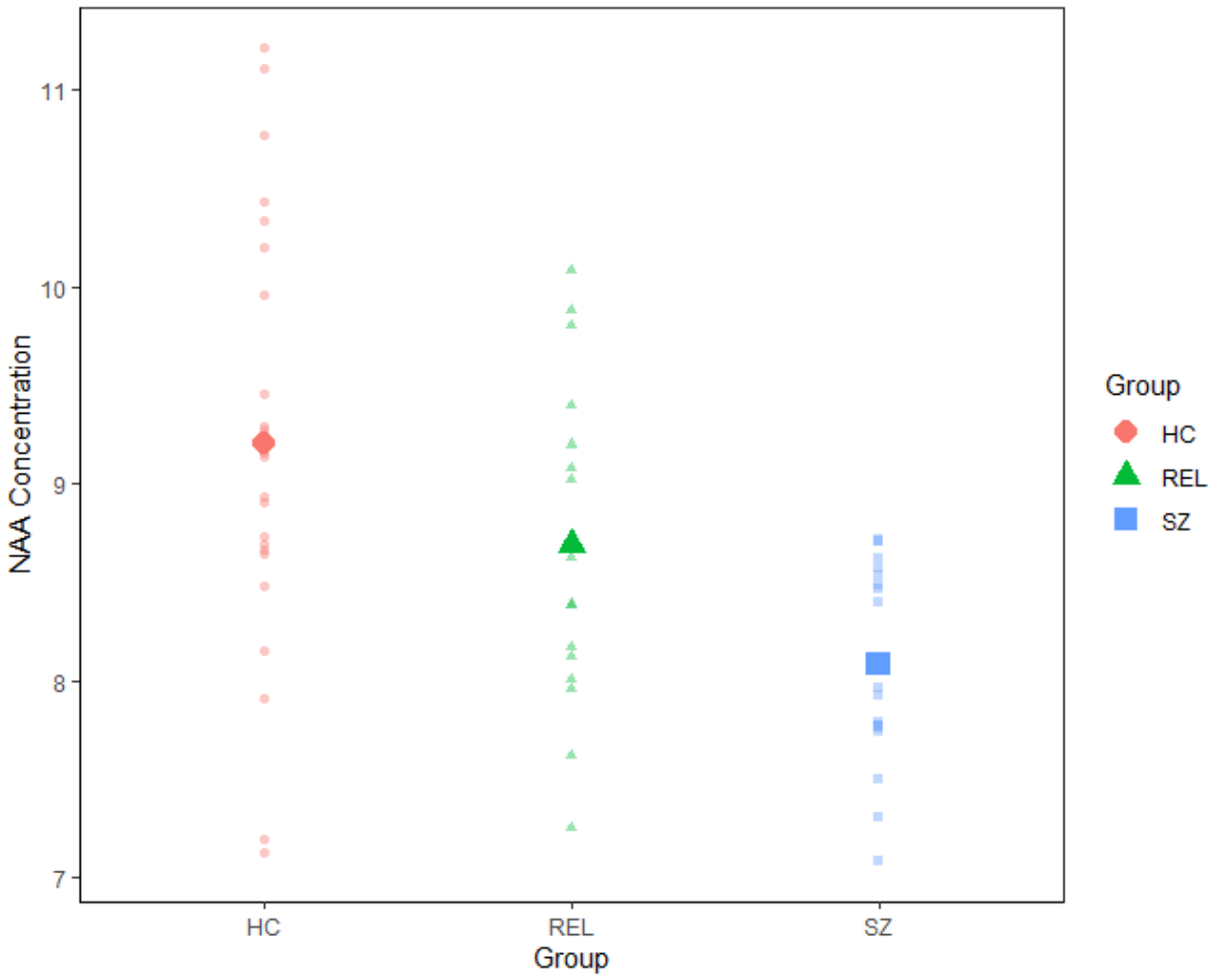


*Note: NAA concentrations listed in mMol. HC = red circle, REL = green triangle, SZ = blue squares.*

**Figure 4.**

Estimated concentrations of NAA in the right basal ganglia when controlling for age and % of gray matter

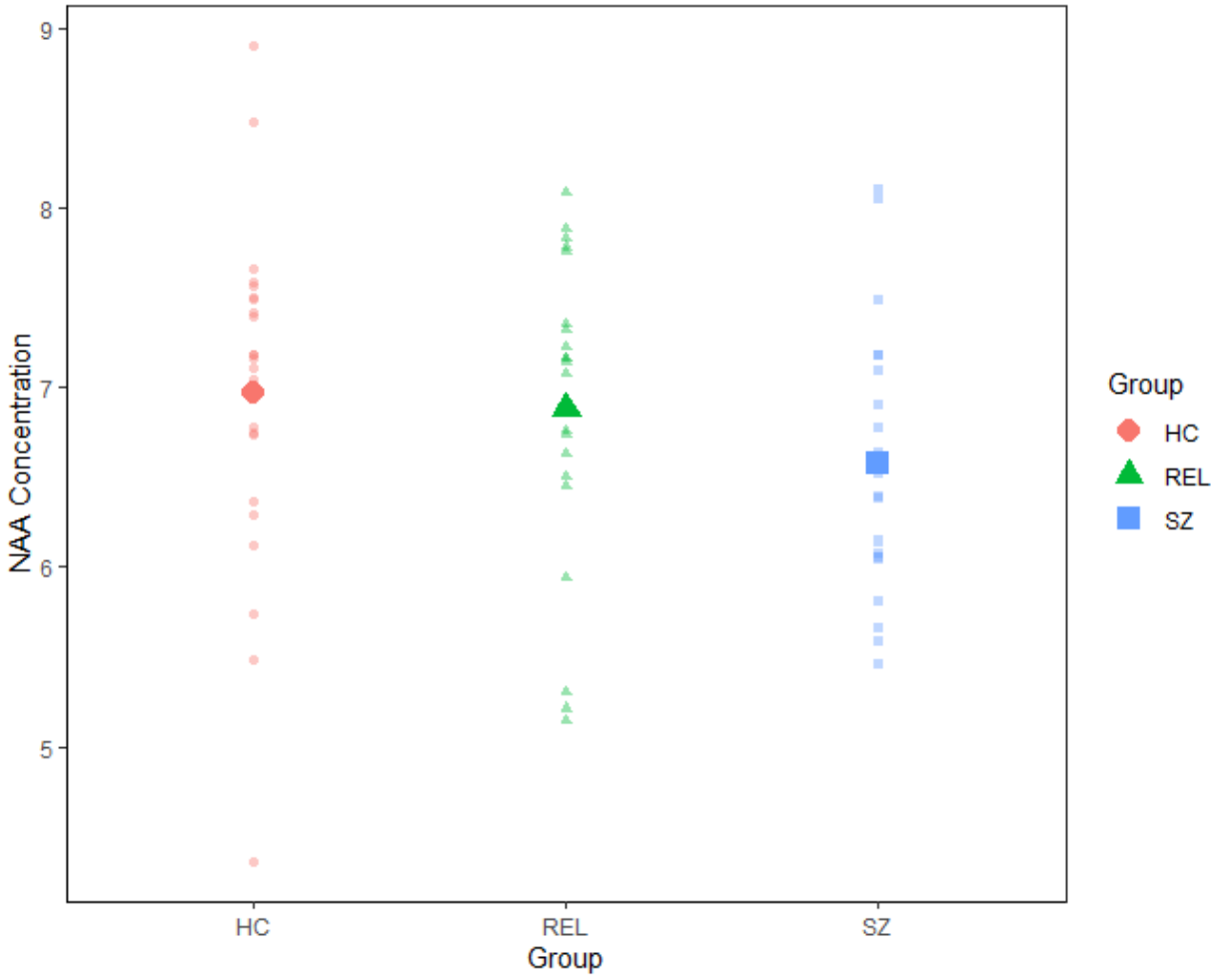


*Note: NAA concentrations listed in mMol. HC = red circle, REL = green triangle, SZ = blue squares.*

**Figure 5.**

Regions in which lower visual cortex NAA concentration predict elevated MD.

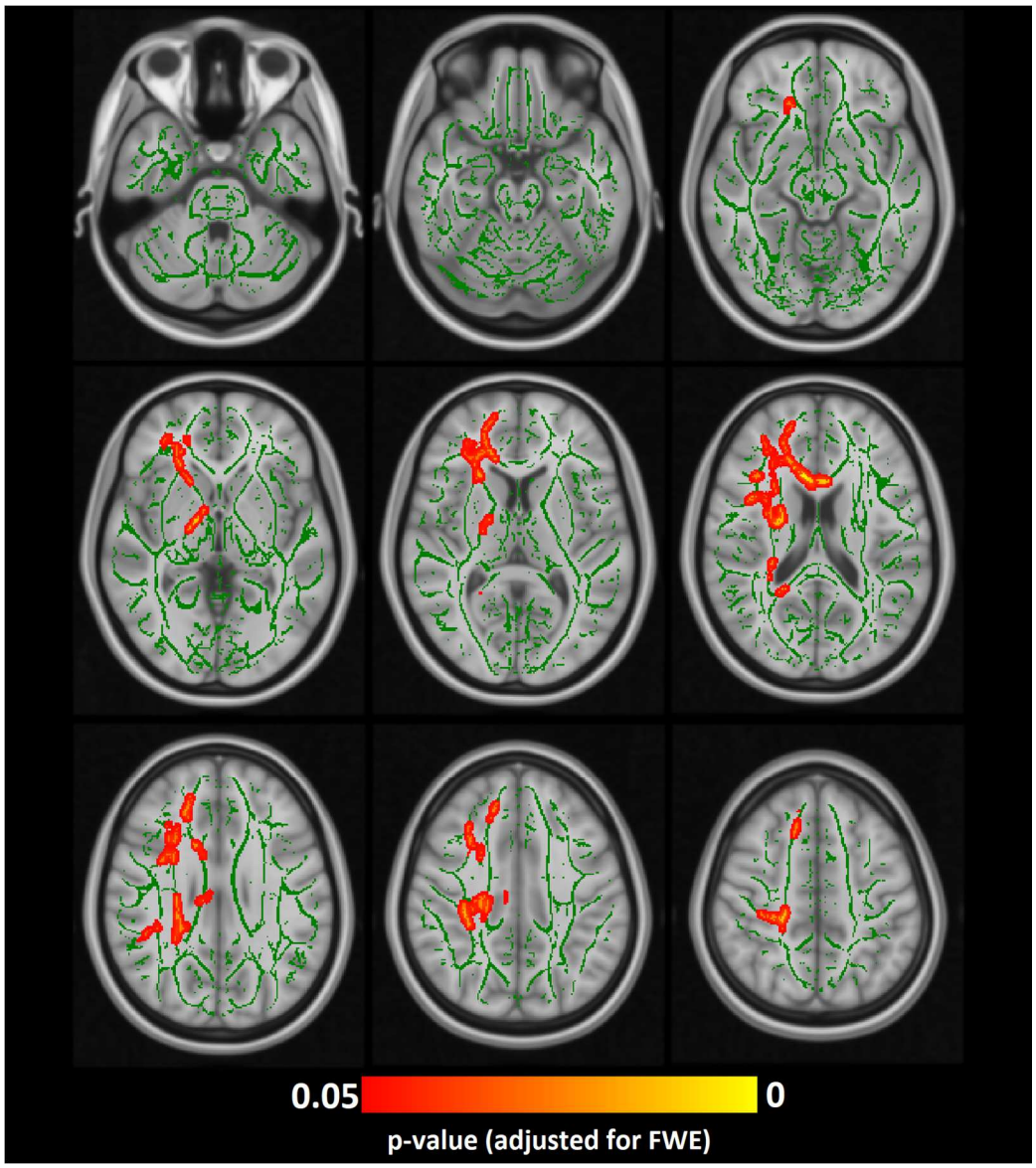


*Note*: *Correlations between NAA concentrations in the visual cortex and mean diffusivity across the entire sample. Significant negative correlations were observed between NAA concentrations in the visual cortex and MD in the right superior longitudinal fasciculus, anterior thalamic radiation, and forceps minor (labelled in red). Results are overlaid on the study-specific whole-group mean white matter skeleton.*

**Figure 6.**

Regions in which lower visual cortex NAA predict elevated RD.

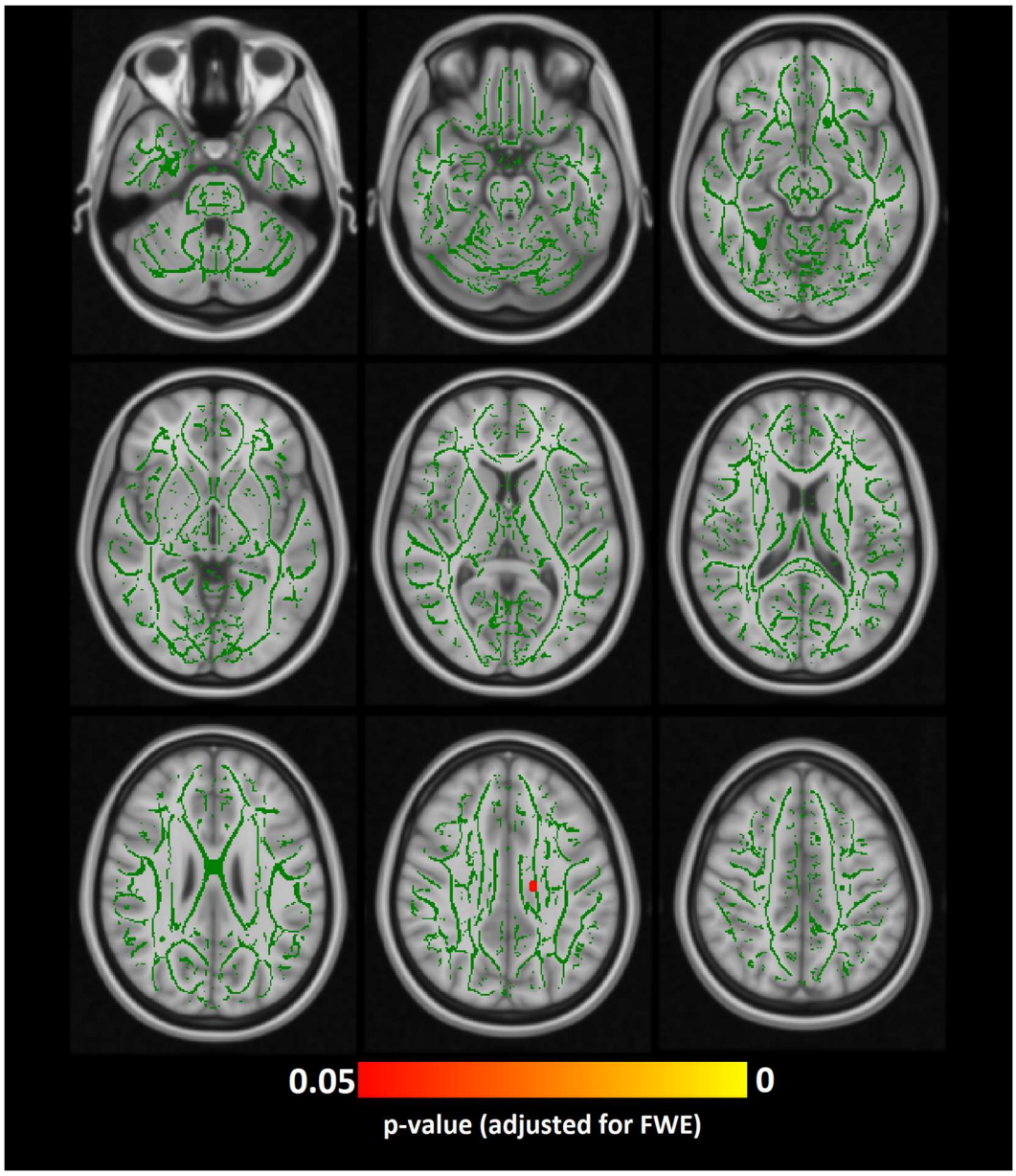


*Note*: *Correlations between NAA concentrations in the visual cortex and radial diffusivity across the entire sample. Significant negative correlations were observed between NAA concentrations in the visual cortex and RD in the superior longitudinal fasciculus (labeled in red). Results are overlaid on the study-specific whole-group mean white matter skeleton.*

**Figure 7.**

Regions in which lower visual cortex NAA concentration predict elevated AD

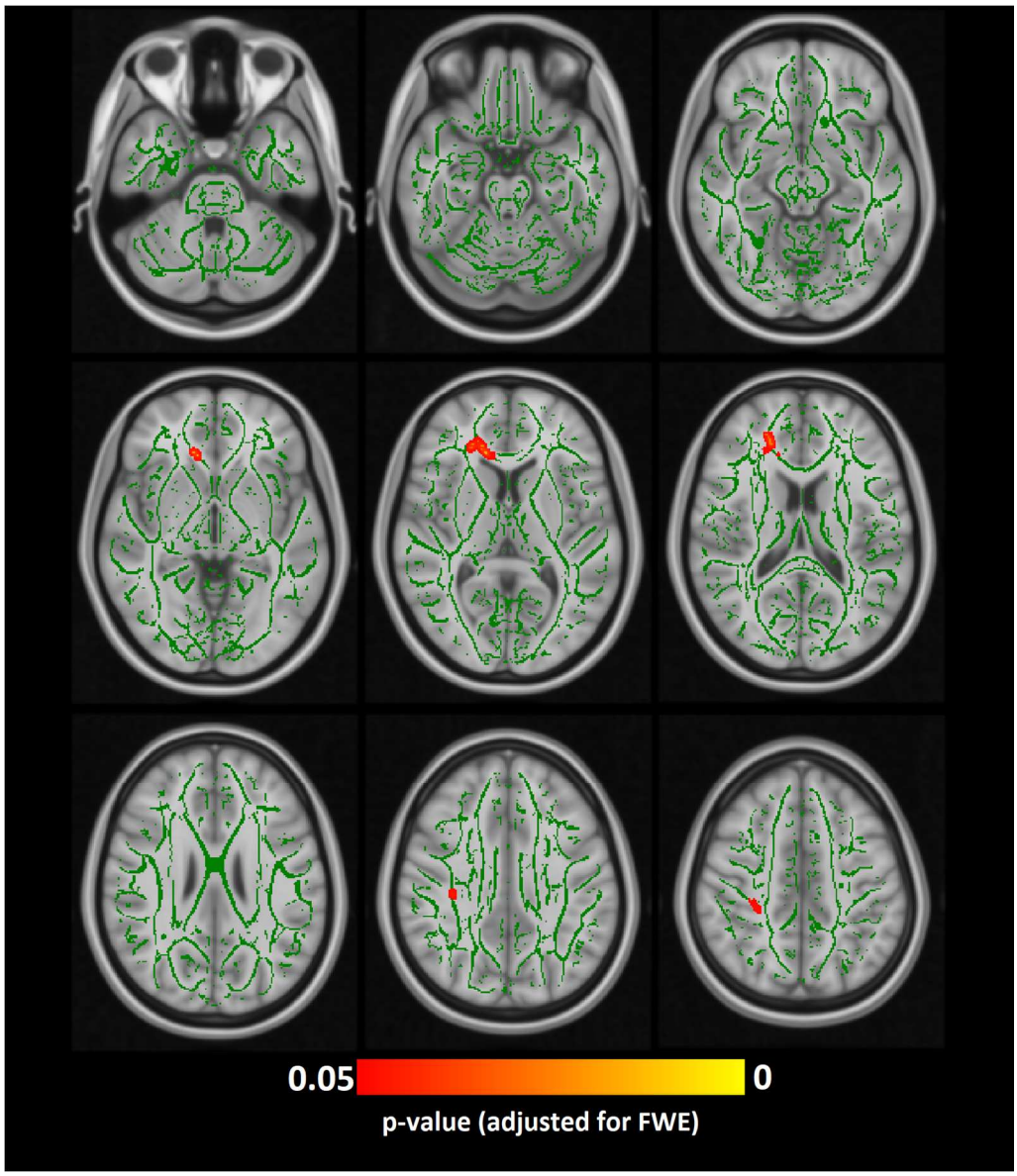


*Note*: *Correlations between NAA concentrations in the visual cortex and axial diffusivity across the entire sample. Significant negative correlations were observed between NAA concentrations in the visual cortex and AD in the right anterior thalamic radiation, forces minor and the right superior longitudinal fasciculus (labeled in red). Results are overlaid on the study-specific whole-group mean white matter skeleton.*

**Figure 8.**

Regions in which higher basal ganglia NAA concentration predict elevated FA

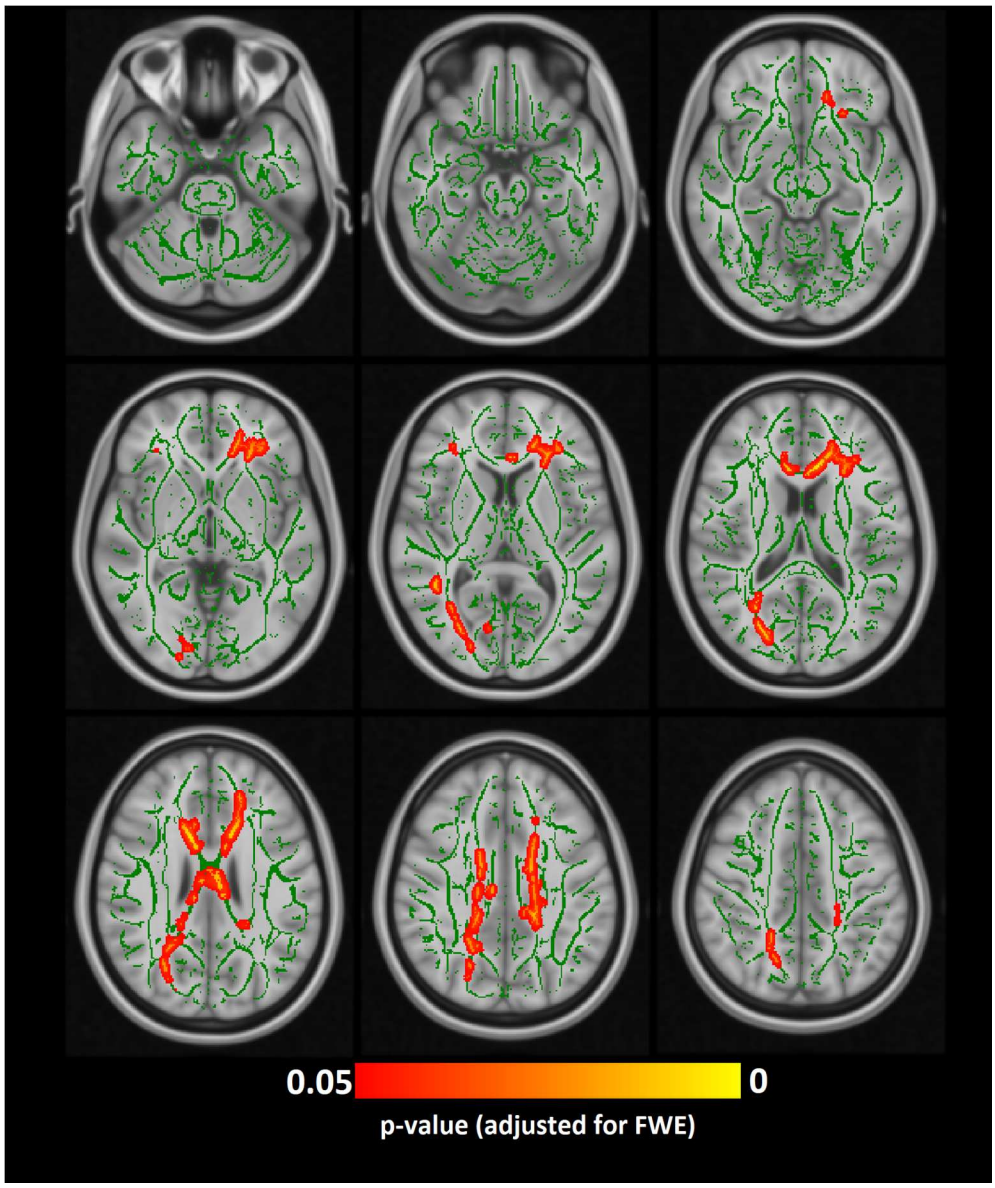


*Note*: *Correlations between NAA concentrations in the right basal ganglia and fractional anisotropy across the entire sample. Significant positive correlations were observed between NAA concentrations in the right basal ganglia and FA in the right inferior front-occipital fasciculus, right anterior thalamic radiation, and the right superior longitudinal fasciculus (labeled in red). Results are overlaid on the study-specific whole-group mean white matter skeleton.*

**Figure 9.**

Regions in which lower basal ganglia NAA concentration predict increased RD

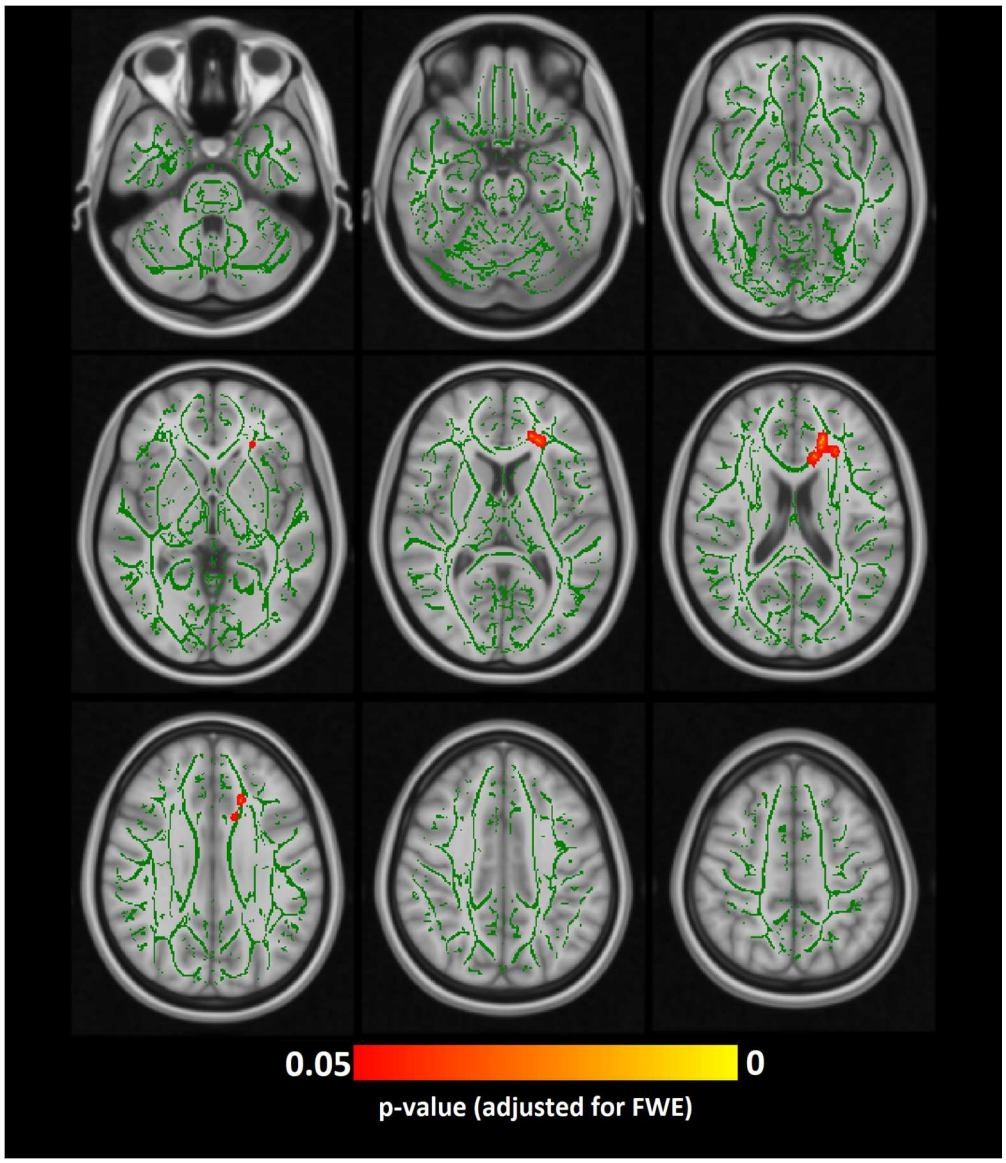


*Note*: *Correlations between NAA concentrations in the right basal ganglia and radial diffusivity across the entire sample. Significant negative correlations were observed between NAA concentrations in the right basal ganglia and RD in the forceps minor and the left anterior thalamic radiation (labeled in red). Results are overlaid on the study-specific whole-group mean white matter skeleton.*

**Figure 10.**

Regions in which lower basal ganglia NAA concentration predict increased AD

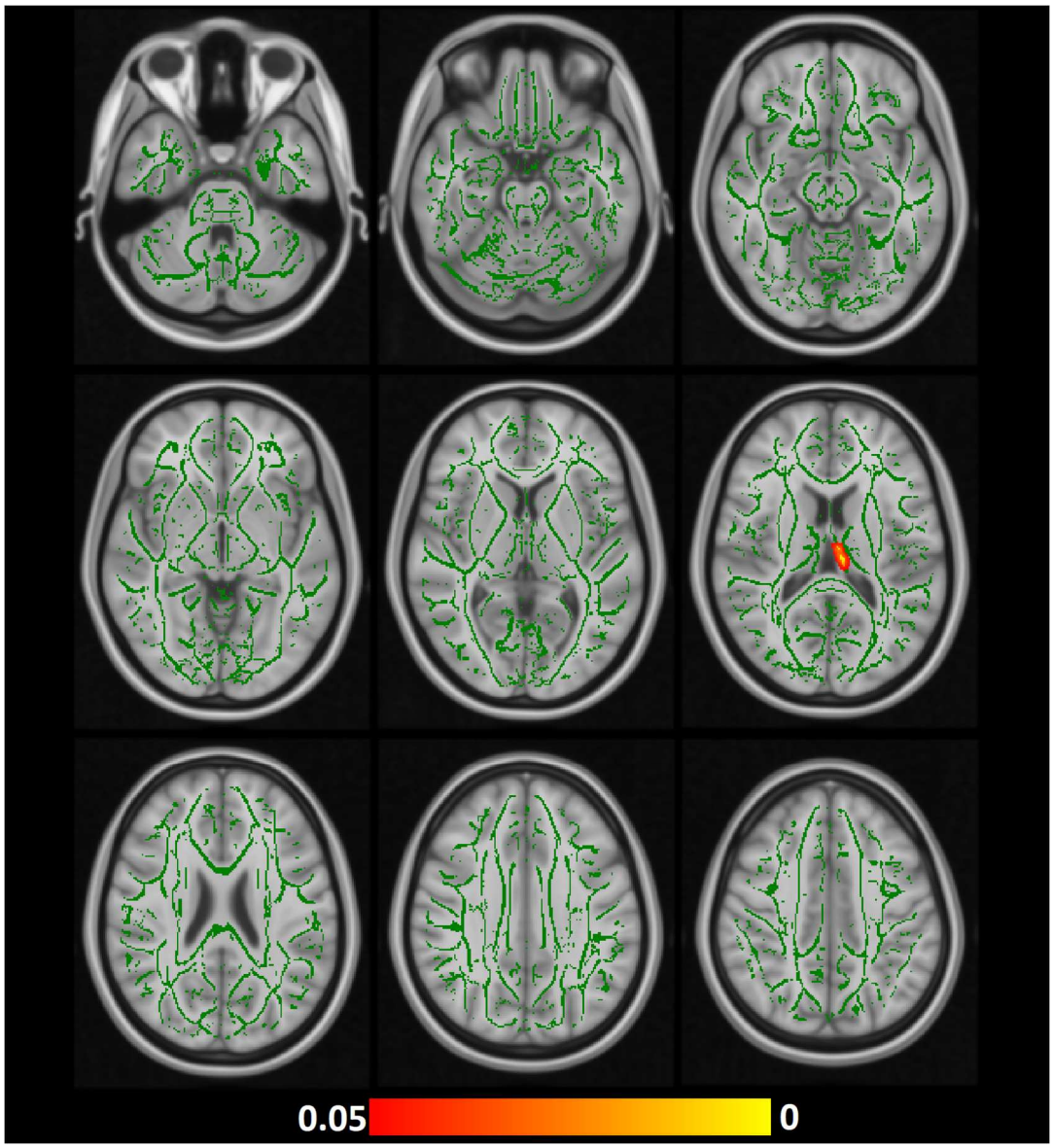


*Note*: *Correlations between NAA concentrations in the right basal ganglia and radial diffusivity across the entire sample. Significant negative correlations were observed between NAA concentrations in the right basal ganglia and AD in the left anterior thalamic radiation (labeled in red). Results are overlaid on the study-specific whole-group mean white matter skeleton.*

# REFERENCES

## REFERENCES


Andersson, J. L. R., & Skare, S. (2002). A model-based method for retrospective correction of geometric distortions in diffusion-weighted EPI. *NeuroImage*, *16*(1), 177–199. https://doi.org/10.1006/nimg.2001.1039

Andersson, J. L. R., Jenkinson, M. & Smith, S. (2007a). Non-linear optimisation. *FMRIB technical rpeort TR07JA1* from www.fmrib.ox.ac.uk/analysis/techrep

Andersson, J. L. R., Jenkinson, M. & Smith, S. (2007a). Non-linear registration, aka spatial normalisation. *FMRIB technical report TR07JA2* from www.fmrib.ox.ac.uk/analysis/techrep

Andreasen, N. C., Flaum, M., & Arndt, S. (1992). The Comprehensive Assessment of Symptoms and History (CASH): an instrument for assessing diagnosis and psychopathology. *Archives of general psychiatry*, *49*(8), 615-623.

Ashburner, J., & Friston, K. J. (2005). Unified segmentation. Neuroimage, 26(3), 839-851.

Aung, W. Y., Mar, S., & Benzinger, T. L. (2013). Diffusion tensor MRI as a biomarker in axonal and myelin damage. *Imaging in Medicine*, *5*(5), 427–440. https://doi.org/10.2217/iim.13.49

Bennett, I. J., Madden, D. J., Vaidya, C. J., Howard, D. V., & Howard, J. H. (2010). Age-related differences in multiple measures of white matter integrity: A diffusion tensor imaging study of healthy aging. *Human Brain Mapping*, *31*(3), 378–390. https://doi.org/10.1002/hbm.20872

Boos, H. B. M., Aleman, A., Cahn, W., Hulshoff Pol, H., & Kahn, R. S. (2007). Brain volumes in relatives of patients with schizophrenia: A meta-analysis. *Archives of General Psychiatry*, *64*(3), 297–304. https://doi.org/10.1001/archpsyc.64.3.297

Brugger, S., Davis, J. M., Leucht, S., & Stone, J. M. (2011). Proton magnetic resonance spectroscopy and illness stage in schizophreniaa systematic review and meta-analysis. *Biological Psychiatry*, *69*(5), 495–503. https://doi.org/10.1016/j.biopsych.2010.10.004

Budde, M. D., Janes, L., Gold, E., Turtzo, L. C., & Frank, J. A. (2011). The contribution of gliosis to diffusion tensor anisotropy and tractography following traumatic brain injury: Validation in the rat using Fourier analysis of stained tissue sections. *Brain*, *134*(8), 2248–2260. https://doi.org/10.1093/brain/awr161

Budde, M. D., Xie, M., Cross, A. H., & Song, S. K. (2009). Axial diffusivity is the primary correlate of axonal injury in the experimental autoimmune encephalomyelitis spinal cord: A quantitative pixelwise analysis. *Journal of Neuroscience*, *29*(9), 2805–2813. https://doi.org/10.1523/JNEUROSCI.4605-08.2009

Camchong, J., Lim, K. O., Sponheim, S. R., & MacDonald, A. W. (2009). Frontal white matter

integrity as an endophenotype for schizophrenia: Diffusion tensor imaging in monozygotic twins and patients' nonpsychotic relatives. *Frontiers in Human Neuroscience*, *3*(OCT), 1–6. https://doi.org/10.3389/neuro.09.035.2009

Campbell, G. R., & Mahad, D. J. (2011). Mitochondria as Crucial Players in Demyelinated Axons: Lessons from Neuropathology and Experimental Demyelination. *Autoimmune Diseases*, *1*(1). https://doi.org/10.4061/2011/262847

Chakraborty, G., Mekala, P., Yahya, D., Wu, G., & Ledeen, R. W. (2001). Intraneuronal N-acetylaspartate supplies acetyl groups for myelin lipid synthesis: Evidence for myelin-associated aspartoacylase. *Journal of Neurochemistry*, *78*(4), 736–745. https://doi.org/10.1046/j.1471-4159.2001.00456.x

Chiappelli, J., Hong, L. E., Wijtenburg, S. A., Du, X., Gaston, F., Kochunov, P., & Rowland, L. M. (2015). Alterations in frontal white matter neurochemistry and microstructure in schizophrenia: Implications for neuroinflammation. *Translational Psychiatry*, *5*(4). https://doi.org/10.1038/tp.2015.43

Choi, J., Dickson, P., Calabrese, E., Chen, S., White, L., Ellingwood, M., & Provenzale, J. M. (2015). Predicting degree of myelination based on diffusion tensor imagining of canines with mucopolysaccharidosis type i. *Neuroradiology Journal*, *28*(6), 562–573. https://doi.org/10.1177/1971400915609351

Cropley, V. L., Klauser, P., Lenroot, R. K., Bruggemann, J., Sundram, S., Bousman, C., Pereira, A., Di Biase, M. A., Weickert, T. W., Weickert, C. S., Pantelis, C., & Zalesky, A. (2017). Accelerated gray and white matter deterioration with age in schizophrenia. *American Journal of Psychiatry*, *174*(3), 286–295. https://doi.org/10.1176/appi.ajp.2016.16050610

D'Adamo, A. F., & Yatsu, F. M. (1966). Acetate metabolism in the nervous system. N-Acetyl-l-Aspartic Acid and the biosynthesis of brain lipids. *Journal of Neurochemistry*, *13*(10), 961–965. https://doi.org/10.1111/j.1471-4159.1966.tb10292.x

de Graaf RA (1998): In Vivo NMR Spectroscopy. Chichester, England: John Wiley & Sons Ltd

de Zwarte, S. M. C., Brouwer, R. M., Agartz, I., Alda, M., Aleman, A., Alpert, K. I., Bearden, C. E., Bertolino, A., Bois, C., Bonvino, A., Bramon, E., Buimer, E. E. L., Cahn, W., Cannon, D. M., Cannon, T. D., Caseras, X., Castro-Fornieles, J., Chen, Q., Chung, Y., … van Haren, N. E. M. (2019). The association between familial risk and brain abnormalities is disease-specific: an ENIGMA–Relatives study of schizophrenia and bipolar disorder. *Biological Psychiatry*. https://doi.org/10.1016/j.biopsych.2019.03.985

Della Nave, R., Ginestroni, A., Diciotti, S., Salvatore, E., Soricelli, A., & Mascalchi, M. (2011). Axial diffusivity is increased in the degenerating superior cerebellar peduncles of Friedreich's ataxia. *Neuroradiology*, *53*(5), 367–372. https://doi.org/10.1007/s00234-010-0807-1

Di Pietro, V., Amorini, A. M., Tavazzi, B., Vagnozzi, R., Logan, A., Lazzarino, G., Signoretti, S., Lazzarino, G., & Belli, A. (2014). The molecular mechanisms affecting N-

acetylaspartate homeostasis following experimental graded traumatic brain injury. *Molecular Medicine*, *20*(1), 147–157. https://doi.org/10.2119/molmed.2013.00153

Du, F., Cooper, A. J., Thida, T., Shinn, A. K., Cohen, B. M., & Öngür, D. (2013). Myelin and axon abnormalities in schizophrenia measured with magnetic resonance imaging techniques. *Biological Psychiatry*, *74*(6), 451–457. https://doi.org/10.1016/j.biopsych.2013.03.003

Ellison-Wright, I., & Bullmore, E. (2010). Anatomy of bipolar disorder and schizophrenia: A meta-analysis. *Schizophrenia Research*, *117*(1), 1–12. https://doi.org/10.1016/j.schres.2009.12.022

Ernst, T., Kreis, R., & Ross, B. D. (1993). Absolute Quantitation of Water and Metabolites in the Human Brain. I. Compartments and Water. In *Journal of Magnetic Resonance, Series B* (Vol. 102, Issue 1, pp. 1–8). https://doi.org/10.1006/jmrb.1993.1055

Flynn, S. W., Lang, D. J., Mackay, A. L., Goghari, V., Vavasour, I. M., Whittall, K. P., Smith, G. N., Arango, V., Mann, J. J., Dwork, A. J., Falkai, P., & Honer, W. G. (2003). Abnormalities of myelination in schizophrenia detected in vivo with MRI, and post-mortem with analysis of oligodendrocyte proteins. *Molecular Psychiatry*, *8*(9), 811–820. https://doi.org/10.1038/sj.mp.4001337

Friston, K. J. (1998). The disconnection hypothesis. *Schizophrenia research*, *30*(2), 115-125.

Fuente-Sandoval, C. D. La, León-Ortiz, P., Favila, R., Stephano, S., Mamo, D., Ramírez-Bermdez, J., & Graff-Guerrero, A. (2011). Higher levels of glutamate in the associative-striatum of subjects with prodromal symptoms of schizophrenia and patients with first-episode psychosis. *Neuropsychopharmacology*, *36*(9), 1781–1791. https://doi.org/10.1038/npp.2011.65

Ghosh, N., Holshouser, B., Oyoyo, U., Barnes, S., Tong, K., & Ashwal, S. (2017). Combined Diffusion Tensor and Magnetic Resonance Spectroscopic Imaging Methodology for Automated Regional Brain Analysis: Application in a Normal Pediatric Population. *Developmental Neuroscience*, *39*(5), 413–429. https://doi.org/10.1159/000475545

Gracitelli, C. P. B., Abe, R. Y., Diniz-Filho, A., Vaz-de-Lima, F. B., Paranhos, A., & Medeiros, F. A. (2015). Ophthalmology Issues in Schizophrenia. *Current Psychiatry Reports*, *17*(5), 1–20. https://doi.org/10.1007/s11920-015-0569-x

Grošić, V., Grošić, P. F., Kalember, P., Janović, M. B., Radoš, M., Mihanović, M., & Henigsberg, N. (2014). The effect of atypical antipsychotics on brain N-acetylaspartate levels in antipsychotic-naïve first-episode patients with schizophrenia: A preliminary study. *Neuropsychiatric Disease and Treatment*, *10*, 1243–1253. https://doi.org/10.2147/NDT.S61415

Habtewold, T. D., Rodijk, L. H., Liemburg, E. J., Sidorenkov, G., Boezen, H. M., Bruggeman, R., & Alizadeh, B. Z. (2020). A systematic review and narrative synthesis of data-driven studies in schizophrenia symptoms and cognitive deficits. *Translational Psychiatry*, *10*(1).

https://doi.org/10.1038/s41398-020-00919-x

Haijma, S. V., Van Haren, N., Cahn, W., Koolschijn, P. C. M. P., Hulshoff Pol, H. E., & Kahn, R. S. (2013). Brain volumes in schizophrenia: A meta-analysis in over 18 000 subjects. *Schizophrenia Bulletin*, *39*(5), 1129–1138. https://doi.org/10.1093/schbul/sbs118

Hannoun, S., Bagory, M., Durand-Dubief, F., Ibarrola, D., Comte, J. C., Confavreux, C., Cotton, F., & Sappey-Marinier, D. (2012). Correlation of diffusion and metabolic alterations in different clinical forms of multiple sclerosis. *PLoS ONE*, *7*(3). https://doi.org/10.1371/journal.pone.0032525

Hjorthøj, C., Stürup, A. E., McGrath, J. J., & Nordentoft, M. (2017). Years of potential life lost and life expectancy in schizophrenia: a systematic review and meta-analysis. *The Lancet Psychiatry*, *4*(4), 295–301. https://doi.org/10.1016/S2215-0366(17)30078-0

Hope, T. R., Selnes, P., Rektorová, I., Anderkova, L., Nemcova-Elfmarkova, N., Balážová, Z., Dale, A., Bjørnerud, A., & Fladby, T. (2019). Diffusion tensor and restriction spectrum imaging reflect different aspects of neurodegeneration in Parkinson's disease. *PLoS ONE*, *14*(5), 1–13. https://doi.org/10.1371/journal.pone.0217922

Iwata, Y., Nakajima, S., Plitman, E., Mihashi, Y., Caravaggio, F., Chung, J. K., Kim, J., Gerretsen, P., Mimura, M., Remington, G., & Graff-Guerrero, A. (2018). Neurometabolite levels in antipsychotic-naïve/free patients with schizophrenia: A systematic review and meta-analysis of 1 H-MRS studies. In *Progress in Neuro-Psychopharmacology and Biological Psychiatry* (Vol. 86, Issue January, pp. 340–352). https://doi.org/10.1016/j.pnpbp.2018.03.016

Jääskeläinen, E., Juola, P., Hirvonen, N., McGrath, J. J., Saha, S., Isohanni, M., Veijola, J., & Miettunen, J. (2013). A systematic review and meta-analysis of recovery in schizophrenia. *Schizophrenia Bulletin*, *39*(6), 1296–1306. https://doi.org/10.1093/schbul/sbs130

Kay, S. R., Opler, L. A., & Lindenmayer, J. P. (1989). The Positive and Negative Syndrome Scale (PANSS): rationale and standardisation. *The British Journal of Psychiatry. Supplement*, *13*(7), 59–67.

Kelly, S., Jahanshad, N., Zalesky, A., Kochunov, P., Agartz, I., Alloza, C., Andreassen, O. A., Arango, C., Banaj, N., Bouix, S., Bousman, C. A., Brouwer, R. M., Bruggemann, J., Bustillo, J., Cahn, W., Calhoun, V., Cannon, D., Carr, V., Catts, S., … Donohoe, G. (2018). Widespread white matter microstructural differences in schizophrenia across 4322 individuals: Results from the ENIGMA Schizophrenia DTI Working Group. *Molecular Psychiatry*, *23*(5), 1261–1269. https://doi.org/10.1038/mp.2017.170

Keshavan, M. S., Dick, R. M., Diwadkar, V. A., Montrose, D. M., Prasad, K. M., & Stanley, J. A. (2009). Striatal metabolic alterations in non-psychotic adolescent offspring at risk for schizophrenia: A 1H spectroscopy study. *Schizophrenia Research*, *115*(1), 88–93. https://doi.org/10.1016/j.schres.2009.08.012

Kraguljac, N. V., Reid, M., White, D., Jones, R., den Hollander, J., Lowman, D., & Lahti, A. C.

(2012). Neurometabolites in schizophrenia and bipolar disorder - A systematic review and meta-analysis. *Psychiatry Research - Neuroimaging*, *203*(2–3), 111–125. https://doi.org/10.1016/j.pscychresns.2012.02.003

Kreis, R. (2016). The trouble with quality filtering based on relative Cramér-Rao lower bounds. *Magnetic Resonance in Medicine*, *75*(1), 15–18. https://doi.org/10.1002/mrm.25568

Kronlage, M., Pitarokoili, K., Schwarz, D., Godel, T., Heiland, S., Yoon, M. S., Bendszus, M., & Bäumer, P. (2017). Diffusion Tensor Imaging in Chronic Inflammatory Demyelinating Polyneuropathy: Diagnostic Accuracy and Correlation with Electrophysiology. *Investigative Radiology*, *52*(11), 701–707. https://doi.org/10.1097/RLI.0000000000000394

Lang, D. J. M., Yip, E., Mackay, A. L., Thornton, A. E., Vila-Rodriguez, F., Macewan, G. W., Kopala, L. C., Smith, G. N., Laule, C., Macrae, C. B., & Honer, W. G. (2014). 48 echo T2 myelin imaging of white matter in first-episode schizophrenia: Evidence for aberrant myelination. *NeuroImage: Clinical*, *6*, 408–414. https://doi.org/10.1016/j.nicl.2014.10.006

Marjańska, M., Auerbach, E. J., Valabrègue, R., Van de Moortele, P. F., Adriany, G., & Garwood, M. (2012). Localized 1H NMR spectroscopy in different regions of human brain in vivo at 7T: T 2 relaxation times and concentrations of cerebral metabolites. *NMR in Biomedicine*, *25*(2), 332–339. https://doi.org/10.1002/nbm.1754

Marsman, A., Van Den Heuvel, M. P., Klomp, D. W. J., Kahn, R. S., Luijten, P. R., & Hulshoff Pol, H. E. (2013). Glutamate in schizophrenia: A focused review and meta-analysis of 1H-MRS studies. In *Schizophrenia Bulletin* (Vol. 39, Issue 1, pp. 120–129). https://doi.org/10.1093/schbul/sbr069

Matthews, P. R., Eastwood, S. L., & Harrison, P. J. (2012). Reduced myelin basic protein and actin-related gene expression in visual cortex in schizophrenia. *PLoS ONE*, *7*(6). https://doi.org/10.1371/journal.pone.0038211

Moffett, J. R., Arun, P., Ariyannur, P. S., & Namboodiri, A. M. A. (2013). N-Acetylaspartate reductions in brain injury: Impact on post-injury neuroenergetics, lipid synthesis, and protein acetylation. *Frontiers in Neuroenergetics*, *5*(DEC), 1–19. https://doi.org/10.3389/fnene.2013.00011

Moffett, J. R., Ross, B., Arun, P., Madhavarao, C. N., & Namboodiri, A. M. A. (2007). N-Acetylaspartate in the CNS: From neurodiagnostics to neurobiology. *Progress in Neurobiology*, *81*(2), 89–131. https://doi.org/10.1016/j.pneurobio.2006.12.003

Mondino, M., Brunelin, J., & Saoud, M. (2013). N-acetyl-aspartate level is decreased in the prefrontal cortex in subjects at-risk for schizophrenia. *Frontiers in Psychiatry*, *4*(SEP), 1–6. https://doi.org/10.3389/fpsyt.2013.00099

Mori, S., Oishi, K., Jiang, H., Jiang, L., Li, X., Akhter, K., ... & Mazziotta, J. (2008). Stereotaxic white matter atlas based on diffusion tensor imaging in an ICBM template. *Neuroimage, 40*(2), 570-582.

Near, J. (2013). Spectral Quantification and Pitfalls in Interpreting Magnetic Resonance Spectroscopic Data. What To Look Out For. In *Magnetic Resonance Spectroscopy: Tools for Neuroscience Research and Emerging Clinical Applications* (pp. 49–67). Elsevier Inc. https://doi.org/10.1016/B978-0-12-401688-0.00005-7

Nickel, M., & Gu, C. (2018). Regulation of central nervous system myelination in higher brain functions. *Neural Plasticity*, *2018*. https://doi.org/10.1155/2018/6436453

Oldfield, R. C. (1971). The assessment and analysis of handedness: The Edinburgh inventory. *Neuropsychologia*, *9*(1), 97–113. https://doi.org/10.1016/0028-3932(71)90067-4

Oishi, K., Zilles, K., Amunts, K., Faria, A., Jiang, H., Li, X., ... & Mori, S. (2008). Human brain white matter atlas: identification and assignment of common anatomical structures in superficial white matter. *Neuroimage, 43*(3), 447-457.

Patel, K. R., Cherian, J., Gohil, K., & Atkinson, D. (2014). Schizophrenia: Overview and treatment options. *P and T*, *39*(9), 638–645.

Patel, T. B., & Clark, J. B. (1979). Synthesis of N-acetyl-L-aspartate by rat brain mitochondria and its involvement in mitochondrial/cytosolic carbon transport. *Biochemical Journal*, *184*(3), 539–546. https://doi.org/10.1042/bj1840539

Pfeuffer J, Tkác I, Provencher SW, Gruetter R (1999): Toward an in vivo neurochemical profile: Quantification of 18 metabolites in short-echo time (1)H NMR spectra of the rat brain. J Magn Reson 141: 104–120.

Pierpaoli, C., & Basser, P. J. (1996). Toward a quantitative assessment of diffusion anisotropy. *Magnetic Resonance in Medicine*, *36*(6), 893–906. https://doi.org/10.1002/mrm.1910360612

Prasad, K. M., Upton, C. H., Schirda, C. S., Nimgaonkar, V. L., & Keshavan, M. S. (2015). White matter diffusivity and microarchitecture among schizophrenia subjects and first-degree relatives. *Schizophrenia Research*, *161*(1), 70–75. https://doi.org/10.1016/j.schres.2014.09.045

Reid, M. A., Kraguljac, N. V., Avsar, K. B., White, D. M., den Hollander, J. A., & Lahti, A. C. (2013). Proton magnetic resonance spectroscopy of the substantia nigra in schizophrenia. *Schizophrenia Research*, *147*(2–3), 348–354. https://doi.org/10.1016/j.schres.2013.04.036

Reid, M. A., White, D. M., Kraguljac, N. V., & Lahti, A. C. (2016). A combined diffusion tensor imaging and magnetic resonance spectroscopy study of patients with schizophrenia. *Schizophrenia Research*, *170*(2–3), 341–350. https://doi.org/10.1016/j.schres.2015.12.003

Rosas, H. D., Lee, S. Y., Bender, A. C., Zaleta, A. K., Vangel, M., Yu, P., Fischl, B., Pappu, V., Onorato, C., Cha, J. H., Salat, D. H., & Hersch, S. M. (2010). Altered white matter microstructure in the corpus callosum in Huntington's disease: Implications for cortical "disconnection." *NeuroImage*, *49*(4), 2995–3004. https://doi.org/10.1016/j.neuroimage.2009.10.015

Schmand, B., Bakker, D., Saan, R., & Louman, J. (1991). The Dutch Reading Test for Adults: a measure of premorbid intelligence level. *Tijdschrift voor gerontologie en geriatrie*, *22*(1), 15-19.

Seehaus, A., Roebroeck, A., Bastiani, M., Fonseca, L., Bratzke, H., Lori, N., Vilanova, A., Goebel, R., & Galuske, R. (2015). Histological validation of high-resolution DTI in human post mortem tissue. *Frontiers in Neuroanatomy*, *9*(JULY), 1–12. https://doi.org/10.3389/fnana.2015.00098

Shenton, M. E., Dickey, C. C., Frumin, M., & Mccarley, R. W. (2010). Nihms166514. *Schizophrenia Research*, *49*, 1–52. https://www.ncbi.nlm.nih.gov/pmc/articles/PMC2812015/

Signoretti, S., Marmarou, A., Tavazzi, B., Lazzarino, G., Beaumont, A., & Vagnozzi, R. (2001). and Mitochondrial Dysfunction Following. *Journal of Neurotrauma*, *18*(10), 977–991.

Smith, S. M. (2002). Fast robust automated brain extraction. *Human Brain Mapping*, *17*(3), 143–155. https://doi.org/10.1002/hbm.10062

Smith, S. M., Jenkinson, M., Johansen-Berg, H., Rueckert, D., Nichols, T. E., Mackay, C. E., Watkins, K. E., Ciccarelli, O., Cader, M. Z., Matthews, P. M., & Behrens, T. E. J. (2006). Tract-based spatial statistics: Voxelwise analysis of multi-subject diffusion data. *NeuroImage*, *31*(4), 1487–1505. https://doi.org/10.1016/j.neuroimage.2006.02.024

Smith, S. M., Jenkinson, M., Woolrich, M. W., Beckmann, C. F., Behrens, T. E. J., Johansen-Berg, H., Bannister, P. R., De Luca, M., Drobnjak, I., Flitney, D. E., Niazy, R. K., Saunders, J., Vickers, J., Zhang, Y., De Stefano, N., Brady, J. M., & Matthews, P. M. (2004). Advances in functional and structural MR image analysis and implementation as FSL. *NeuroImage*, *23*(SUPPL. 1), 208–219. https://doi.org/10.1016/j.neuroimage.2004.07.051

Song, S. K., Sun, S. W., Ju, W. K., Lin, S. J., Cross, A. H., & Neufeld, A. H. (2003). Diffusion tensor imaging detects and differentiates axon and myelin degeneration in mouse optic nerve after retinal ischemia. *NeuroImage*, *20*(3), 1714–1722. https://doi.org/10.1016/j.neuroimage.2003.07.005

Song, S. K., Sun, S. W., Ramsbottom, M. J., Chang, C., Russell, J., & Cross, A. H. (2002). Dysmyelination revealed through MRI as increased radial (but unchanged axial) diffusion of water. *NeuroImage*, *17*(3), 1429–1436. https://doi.org/10.1006/nimg.2002.1267

Steel, R. M., Bastin, M. E., McConnell, S., Marshall, I., Cunningham-Owens, D. G., Lawrie, S. M., Johnstone, E. C., & Best, J. J. K. (2001). Diffusion tensor imaging (DTI) and proton magnetic resonance spectroscopy (1H MRS) in schizophrenic subjects and normal controls. *Psychiatry Research - Neuroimaging*, *106*(3), 161–170. https://doi.org/10.1016/S0925-4927(01)00080-4

Steen, R. G., Hamer, R. M., & Lieberman, J. A. (2005). Measurement of brain metabolites by 1H magnetic resonance spectroscopy in patients with schizophrenia: A systematic review and meta-analysis. *Neuropsychopharmacology*, *30*(11), 1949–1962.

https://doi.org/10.1038/sj.npp.1300850

Stephan, K. E., Friston, K. J., & Frith, C. D. (2009). Dysconnection in Schizophrenia: From abnormal synaptic plasticity to failures of self-monitoring. *Schizophrenia Bulletin*, *35*(3), 509–527. https://doi.org/10.1093/schbul/sbn176

Stolp, H. B., Ball, G., So, P. W., Tournier, J. D., Jones, M., Thornton, C., & Edwards, A. D. (2018). Voxel-wise comparisons of cellular microstructure and diffusion-MRI in mouse hippocampus using 3D Bridging of Optically-clear histology with Neuroimaging Data (3D-BOND). *Scientific Reports*, *8*(1), 1–12. https://doi.org/10.1038/s41598-018-22295-9

Sun, S. W., Liang, H. F., Le, T. Q., Armstrong, R. C., Cross, A. H., & Song, S. K. (2006). Differential sensitivity of in vivo and ex vivo diffusion tensor imaging to evolving optic nerve injury in mice with retinal ischemia. *NeuroImage*, *32*(3), 1195–1204. https://doi.org/10.1016/j.neuroimage.2006.04.212

Tandon, N., Bolo, N. R., Sanghavi, K., Mathew, I. T., Francis, A. N., Stanley, J. A., & Keshavan, M. S. (2013). Brain metabolite alterations in young adults at familial high risk for schizophrenia using proton magnetic resonance spectroscopy. *Schizophrenia Research*, *148*(1–3), 59–66. https://doi.org/10.1016/j.schres.2013.05.024

Tang, C. Y., Friedman, J., Shungu, D., Chang, L., Ernst, T., Stewart, D., Hajianpour, A., Carpenter, D., Ng, J., Mao, X., Hof, P. R., Buchsbaum, M. S., Davis, K., & Gorman, J. M. (2007). Correlations between Diffusion Tensor Imaging (DTI) and Magnetic Resonance Spectroscopy (1H MRS) in schizophrenic patients and normal controls. *BMC Psychiatry*, *7*, 1–11. https://doi.org/10.1186/1471-244X-7-25

Thakkar, K. N., Rösler, L., Wijnen, J. P., Boer, V. O., Klomp, D. W. J., Cahn, W., Kahn, R. S., & Neggers, S. F. W. (2017). 7T Proton Magnetic Resonance Spectroscopy of Gamma-Aminobutyric Acid, Glutamate, and Glutamine Reveals Altered Concentrations in Patients With Schizophrenia and Healthy Siblings. *Biological Psychiatry*, *81*(6), 525–535. https://doi.org/10.1016/j.biopsych.2016.04.007

Tohid, H., Faizan, M., & Faizan, U. (2015). Alterations of the occipital lobe in schizophrenia. *Neurosciences*, *20*(3), 213–224. https://doi.org/10.17712/nsj.2015.3.20140757

Uranova, N. A., Vostrikov, V. M., Orlovskaya, D. D., & Rachmanova, V. I. (2004). Oligodendroglial density in the prefrontal cortex in schizophrenia and mood disorders: A study from the Stanley Neuropathology Consortium. *Schizophrenia Research*, *67*(2–3), 269–275. https://doi.org/10.1016/S0920-9964(03)00181-6

Uranova, N. A., Vostrikov, V. M., Vikhreva, O. V., Zimina, I. S., Kolomeets, N. S., & Orlovskaya, D. D. (2007). The role of oligodendrocyte pathology in schizophrenia. *International Journal of Neuropsychopharmacology*, *10*(4), 537–545. https://doi.org/10.1017/S1461145707007626

Vanes, L. D., Mouchlianitis, E., Barry, E., Patel, K., Wong, K., & Shergill, S. S. (2019). Cognitive correlates of abnormal myelination in psychosis. *Scientific Reports*, *9*(1), 1–9.

https://doi.org/10.1038/s41598-019-41679-z

Vanes, L. D., Mouchlianitis, E., Wood, T. C., & Shergill, S. S. (2018). White matter changes in treatment refractory schizophrenia: Does cognitive control and myelination matter? *NeuroImage: Clinical*, *18*(January), 186–191. https://doi.org/10.1016/j.nicl.2018.01.010

Vitolo, E., Tatu, M. K., Pignolo, C., Cauda, F., Costa, T., Ando, A., & Zennaro, A. (2017). White matter and schizophrenia: A meta-analysis of voxel-based morphometry and diffusion tensor imaging studies. *Psychiatry Research - Neuroimaging*, *270*(September), 8–21. https://doi.org/10.1016/j.pscychresns.2017.09.014

Walker, C. K., Roche, J. K., Sinha, V., & Roberts, R. C. (2018). Substantia nigra ultrastructural pathology in schizophrenia. *Schizophrenia Research*, *197*(2018), 209–218. https://doi.org/10.1016/j.schres.2017.12.004

Whitehurst, T. S., Osugo, M., Townsend, L., Shatalina, E., Vava, R., Onwordi, E. C., & Howes, O. (2020). Proton Magnetic Resonance Spectroscopy of N-acetyl Aspartate in Chronic Schizophrenia, First Episode of Psychosis and High-Risk of Psychosis: A Systematic Review and Meta-Analysis. *Neuroscience and Biobehavioral Reviews*, *119*(September), 255–267. https://doi.org/10.1016/j.neubiorev.2020.10.001

Wing, J. K., Babor, T., Brugha, T. S., Burke, J., Cooper, J. E., Giel, R., ... & Sartorius, N. (1990). SCAN: schedules fonr clinical assessment in neuropsychiatry. *Archives of general psychiatry*, *47*(6), 589-593.

Winkler, A. M., Ridgway, G. R., Webster, M. A., Smith, S. M., & Nichols, T. E. (2014). Permutation inference for the general linear model. *NeuroImage*, *92*, 381–397. https://doi.org/10.1016/j.neuroimage.2014.01.060

Wolfers, T., Doan, N. T., Kaufmann, T., Alnæs, D., Moberget, T., Agartz, I., Buitelaar, J. K., Ueland, T., Melle, I., Franke, B., Andreassen, O. A., Beckmann, C. F., Westlye, L. T., & Marquand, A. F. (2018). Mapping the Heterogeneous Phenotype of Schizophrenia and Bipolar Disorder Using Normative Models. *JAMA Psychiatry*, *75*(11), 1146–1155. https://doi.org/10.1001/jamapsychiatry.2018.2467

Yang, X., Cao, D., Liang, X., & Zhao, J. (2017). Schizophrenia symptomatic associations with diffusion tensor imaging measured fractional anisotropy of brain: a meta-analysis. *Neuroradiology*, *59*(7), 699–708. https://doi.org/10.1007/s00234-017-1844-9

Yao, B., Neggers, S. F. W., Kahn, R. S., & Thakkar, K. N. (2020). Altered thalamocortical structural connectivity in persons with schizophrenia and healthy siblings. *NeuroImage: Clinical*, *28*(December 2019), 102370. https://doi.org/10.1016/j.nicl.2020.102370

Yao, L., Lui, S., Liao, Y., Du, M. Y., Hu, N., Thomas, J. A., & Gong, Q. Y. (2013). White matter deficits in first episode schizophrenia: An activation likelihood estimation meta-analysis. *Progress in Neuro-Psychopharmacology and Biological Psychiatry*, *45*, 100–106. https://doi.org/10.1016/j.pnpbp.2013.04.019